

Smooth and probabilistic PARAFAC model with auxiliary covariates

Leying Guan

Department of Biostatistics, Yale University

August 30, 2022

Abstract

In immunological and clinical studies, matrix-valued time-series data clustering is increasingly popular. Researchers are interested in finding low-dimensional embedding of subjects based on potentially high-dimensional longitudinal features and investigating relationships between static clinical covariates and the embedding. These studies are often challenging due to high dimensionality, as well as the sparse and irregular nature of sample collection along the time dimension. We propose a smoothed probabilistic PARAFAC model with covariates (SPACO) to tackle these two problems while utilizing auxiliary covariates of interest. We provide intensive simulations to test different aspects of SPACO and demonstrate its use on an immunological data set from patients with SARs-CoV-2 infection.

Keywords: Tensor decomposition; Time series; Missing data; Probabilistic model.

1 Introduction

Sparsely observed multivariate times series data are now common in immunological studies. For each subject or participant i ($i = 1, \dots, I$), we can collect multiple measurements on J features over time, but often at n_i different time stamps $\{t_{i,1}, \dots, t_{i,n_i}\}$. For example, for each subject, immune profiles are measured for hundreds of markers at irregular sampling times in Lucas et al. (2020) and Rendeiro et al. (2020). Let $\mathbf{X}_i \in \mathbb{R}^{n_i \times J}$ be the longitudinal measurements for subject i , we can collect \mathbf{X}_i for all I subjects into a sparse three-way tensor $\mathbf{X} \in \mathbb{R}^{I \times T \times J}$, where $T = |\cup_i \{t_{i,1}, \dots, t_{i,n_i}\}|$ is the number of distinct time stamps across all subjects. Since $\{t_{i,1}, \dots, t_{i,n_i}\}$ tend to be small in size and have low overlaps for different subject i , \mathbf{X} may have a high missing rate along the time dimension.

In addition to \mathbf{X}_i , researchers often have a set of nontemporal covariates $\mathbf{z}_i \in \mathbb{R}^q$ for subject i such as medical conditions and demographics, which may account partially for the variation in the temporal measurements \mathbf{X} across subjects. Modeling such auxiliary covariates $\mathbf{Z} := (\mathbf{z}_1, \dots, \mathbf{z}_I)^\top$ together with \mathbf{X} might help with the estimation quality and understanding for the cross-subject heterogeneity.

In this paper, we propose SPACO (smooth and probabilistic PARAFAC model with auxiliary covariates) to adapt to the sparsity long the time dimension in \mathbf{X} and utilize the auxiliary variables \mathbf{Z} . SPACO assumes that \mathbf{X} is a noisy realization of some low-rank signal tensor whose time components are smooth and subject scores have a potential dependence on the auxiliary covariates \mathbf{Z} :

$$x_{itj} = \sum_{k=1}^K u_{ik} \phi_{tk} v_{jk} + \epsilon_{itj}, \quad \epsilon_{itj} \sim \mathcal{N}(0, \sigma_j^2)$$

$$\mathbf{u}_i = (u_{ik})_{k=1}^K \sim \mathcal{N}(\boldsymbol{\eta}_i, \Lambda_f), \quad \boldsymbol{\eta}_i = \boldsymbol{\beta}^\top \mathbf{z}_i.$$

Here, (1) $\boldsymbol{\beta} \in \mathbb{R}^{q \times K}$ describes the dependence of the expected subject score β_i for subject i on \mathbf{z}_i , and (2) u_{ik} , ϕ_{tk} , v_{jk} are the subject score, trajectory value and feature loading for factor k in the PARAFAC model and the observation indexed by (i, t, j) where \mathbf{u}_i has a normal prior $\mathcal{N}(\boldsymbol{\eta}_i, \Lambda_f)$. We impose smoothness on time trajectories $(\phi_{tk})_{t=1}^\top$ and sparsity on $\boldsymbol{\beta}$ to deal with the irregular sampling along the time dimension and potentially high dimensionality in \mathbf{Z} .

Alongside the model proposal, we will also discuss several issues related to SPACO, including model initialization, auto-tuning of smoothness and sparsity in β and hypothesis testing on β through cross-fit. Successfully addressing these issues is crucial to practitioners interested in applying SPACO to their analysis.

In the remaining of the article, we summarize some closely related work in section 1.1 and describe the SPACO model in Section 2 and model parameter estimation with fixed tuning parameters in Section 3. In Section 4, we discuss the aforementioned related issues that could be important in practice. We compare SPACO to several existing methods in Section 5. Finally, in Section 6, we apply SPACO to a highly sparse tensor data set on immunological measurements for SARS-COV-2 infected patients. We provide a python package *SPACO* for researchers interested in applying the proposed method.

1.1 Related work

In the study of multivariate longitudinal data in economics, researchers have combined tensor decomposition with auto-cross-covariance estimation and autoregressive models (Fan et al., 2008; Lam et al., 2011; Fan et al., 2011; Bai and Wang, 2016; Wang et al., 2019, 2021). These approaches do not work well with highly sparse data or do not scale well with the feature dimensions, which are important for working with medical data. Functional PCA (Besse and Ramsay, 1986; Yao et al., 2005) is often used for modeling sparse longitudinal data in the matrix-form. It utilizes the smoothness of time trajectories to handle sparsity in the longitudinal observations, and estimates the eigenvectors and factor scores under this smoothness assumption. Yokota et al. (2016) and Imaizumi and Hayashi (2017) introduced smoothness to tensor decomposition models, and estimated the model parameters by iteratively solving penalized regression problems. The methods above don't consider the auxiliary covariates \mathbf{Z} .

It has been previously discussed that including \mathbf{Z} could potentially improve our estimation. Li et al. (2016) proposed SupSFPC (supervised sparse and functional principal component) and observed that the auxiliary covariates improve the signal estimation quality in the matrix setting for modeling multivariate longitudinal observations. Lock and Li (2018) proposed SupCP which performs supervised multiway factorization model with

complete observation and employs a probabilistic tensor model (Tipping and Bishop, 1999; Mnih and Salakhutdinov, 2007; Hinrich and Mørup, 2019). Although an extension to sparse tensor is straightforward, SupCP does not model the smoothness and can be much more affected by severe missingness along the time dimension.

SPACO can be viewed as an extension of functional PCA and SupSFPC to the setting of three-way tensor decomposition (Acar and Yener, 2008; Sidiropoulos et al., 2017) using the parallel factor (PARAFAC) model (Harshman and Lundy, 1994; Carroll et al., 1980). It uses a probabilistic model and jointly models the smooth longitudinal data with potentially high-dimensional non-temporal covariates \mathbf{Z} . We refer to the SPACO model as SPACO- when no auxiliary covariate \mathbf{Z} is available. SPACO- itself is an attractive alternative to existing tensor decomposition implementations with probabilistic modeling, smoothness regularization, and automatic parameter tuning. In our simulations, we compare SPACO with SPACO to demonstrate the gain from utilizing \mathbf{Z} .

2 SPACO Model

2.1 Notations

Let $\mathbf{X} \in \mathbb{R}^{I \times T \times J}$ be a tensor for some sparse multivariate longitudinal observations, where I is the number of subjects, J is the number of features, and T is the number of total unique time points. For any matrix A , we let $A_{i:}/A_{:,i}$ denote its i^{th} row/column, and often write $A_{:,i}$ as A_i for the i^{th} column for convenience. Let $\mathbf{X}_I := \begin{pmatrix} \mathbf{X}_{:,1} & \cdots & \mathbf{X}_{:,J} \end{pmatrix} \in \mathbb{R}^{I \times (TJ)}$, $\mathbf{X}_T := \begin{pmatrix} \mathbf{X}_{:,1}^\top & \cdots & \mathbf{X}_{:,J}^\top \end{pmatrix} \in \mathbb{R}^{T \times (IJ)}$, $\mathbf{X}_J := \begin{pmatrix} \mathbf{X}_{:,1}^\top & \cdots & \mathbf{X}_{:,T}^\top \end{pmatrix} \in \mathbb{R}^{J \times (IT)}$ be the matrix unfolding of \mathbf{X} in the subject/feature/time dimension respectively. We also define:

Tensor product \odot : $a \in \mathbb{R}^I$, $b \in \mathbb{R}^T$, $c \in \mathbb{R}^J$, then, $A = a \odot b \odot c \in \mathbb{R}^{I \times T \times J}$ with $A_{itj} = a_i b_t c_j$.

Kronecker product \otimes : $A \in \mathbb{R}^{I_1 \times K_1}$, $B \in \mathbb{R}^{I_2 \times K_2}$, then

$$C = A \otimes B = \begin{pmatrix} A_{11}B & \cdots & A_{1K_1}B \\ \vdots & \ddots & \vdots \\ A_{I_11}B & \cdots & A_{I_1K_1}B \end{pmatrix} \in \mathbb{R}^{(I_1 I_2) \times (K_1 K_2)}.$$

Column-wise Khatri-Rao product \odot : $A \in \mathbb{R}^{I_1 \times K}$, $B \in \mathbb{R}^{I_2 \times K}$, then $C = A \odot B \in$

$\mathbb{R}^{(I_1 I_2) \times K}$ with $C_{:,k} = (A_{:,k} \otimes B_{:,k})$ for $k = 1, \dots, K$.

Element-wise multiplication \cdot : $A, B \in \mathbb{R}^{I \times K}$, then $C = A \cdot B \in \mathbb{R}^{I \times K}$ with $C_{ik} = (A_{ik} B_{ik})$; for $b \in \mathbb{R}^K$, $C = A \cdot b = A \text{diag}\{b_1, \dots, b_K\}$; for $b \in \mathbb{R}^I$, $C = b \cdot A = \text{diag}\{b_1, \dots, b_I\} A$.

2.2 smooth and probabilistic PARAFAC model with covariates

We assume \mathbf{X} to be a noisy realization of an underlying signal array $\mathbf{F} = \sum_{k=1}^K \mathbf{U}_k \odot \mathbf{\Phi}_k \odot \mathbf{V}_k$. We stack $\mathbf{U}_k / \mathbf{\Phi}_k / \mathbf{V}_k$ as the columns of $\mathbf{U} / \mathbf{\Phi} / \mathbf{V}$, denote the rows of $\mathbf{U} / \mathbf{\Phi} / \mathbf{V}$ by $\mathbf{u}_i / \phi_t / \mathbf{v}_j$, and their entries by $u_{ik} / \phi_{tk} / v_{jk}$. We let x_{itj} denote the (i, t, j) -entry of \mathbf{X} . Then,

$$x_{itj} = \sum_{k=1}^K u_{ik} \phi_{tk} v_{jk} + \epsilon_{itj}, \quad \mathbf{u}_i \sim \mathcal{N}(\boldsymbol{\eta}_i, \Lambda_f), \quad \epsilon_{ijt} \sim \mathcal{N}(0, \sigma_j^2), \quad (1)$$

where $\Lambda_f = \text{diag}\{s_1^2, \dots, s_K^2\}$ is a $K \times K$ diagonal covariance matrix. Even though \mathbf{X} is often of high rank, we consider the scenario where the rank K of \mathbf{F} is small.

Without covariates, we set the prior mean parameter $\boldsymbol{\eta}_i = \mathbf{0}$. If we are interested in explaining the heterogeneity in $\boldsymbol{\eta}_i$ across subjects with auxiliary covariates $\mathbf{Z} \in \mathbb{R}^{I \times q}$, then we may model $\boldsymbol{\eta}_i$ as a function of $\mathbf{z}_i := \mathbf{Z}_{i,:}$. Here, we consider a linear model $\eta_{ik} = \mathbf{z}_i^\top \boldsymbol{\beta}_k$, $\forall k = 1, \dots, K$. To avoid confusion, we will always call \mathbf{X} the “features”, and \mathbf{Z} the “covariates” or “variables”.

We refer to \mathbf{U} as the subject scores, which characterize differences across subjects and are latent variables. We refer to \mathbf{V} as the feature loadings, which reveal the composition of the factors using the original features and could assist the downstream interpretation. Finally, $\mathbf{\Phi}$ is referred to as the time trajectories, which can be interpreted as function values sampled from some underlying smooth functions $\phi_k(t)$ at a set of discrete-time points, e.g., $\mathbf{\Phi}_k = (\phi_k(t_1), \dots, \phi_k(t_T))$.

Recalling that $\mathbf{X}_I \in \mathbb{R}^{I \times (TJ)}$ is the unfolding of \mathbf{X} in the subject direction, we write \vec{i} for the indices of observed values in the i^{th} row of \mathbf{X}_I , and $\mathbf{X}_{I, \vec{i}}$ for the vector of these observed values. Each such observed value x_{itj} has noise variance σ_j^2 , and we write $\Lambda_{\vec{i}}$ to represent the diagonal covariance matrix with diagonal values σ_j^2 being the corresponding variances for ϵ_{ijt} at indices in \vec{i} . Similarly, we define $\{\vec{t}, \mathbf{X}_{T, \vec{t}}, \Lambda_{\vec{t}}\}$ for the unfolding $\mathbf{X}_T \in \mathbb{R}^{T \times (IJ)}$, and $\{\vec{j}, \mathbf{X}_{J, \vec{j}}, \Lambda_{\vec{j}}\}$ for the observed indices, the associated ob-

served vector and diagonal covariance matrix for the j^{th} row in $\mathbf{X}_J \in \mathbb{R}^{J \times (IT)}$. We set $\Theta = \{\mathbf{V}, \Phi, \beta, (\sigma_j^2, j = 1, \dots, J), (s_k^2, k = 1, \dots, K)\}$ to denote all model parameters. Set $\mathbf{H} = (\mathbf{V} \odot \Phi)$ and $\mathbf{f}_i = \mathbf{X}_{I,\vec{i}} - \mathbf{H}_{\vec{i}} \boldsymbol{\eta}_i$. If \mathbf{U} is observed, the complete data log-likelihood is

$$L(\mathbf{X}, \mathbf{U} | \Theta) = -\frac{1}{2} \sum_i \left(\mathbf{f}_i^\top \Lambda_{\vec{i}}^{-1} \mathbf{f}_i + (\mathbf{u}_i - \boldsymbol{\eta}_i)^\top \Lambda_f^{-1} (\mathbf{u}_i - \boldsymbol{\eta}_i) + \log |\Lambda_{\vec{i}}| + I \log |\Lambda_f| \right). \quad (2)$$

Set $\tilde{\Sigma}_i = \Lambda_{\vec{i}} + \mathbf{H}_{\vec{i}} \Lambda_f \mathbf{H}_{\vec{i}}^\top$. The marginalized log likelihood integrating out the randomness in \mathbf{U} enjoys a closed form (Lock and Li, 2018):

$$L(\mathbf{X} | \Theta) \propto -\frac{1}{2} \left(\sum_i \mathbf{f}_i^\top \tilde{\Sigma}_i^{-1} \mathbf{f}_i + \log |\tilde{\Sigma}_i| \right). \quad (3)$$

Set $\Sigma_i = (\mathbf{H}_{\vec{i}}^\top \Lambda_{\vec{i}}^{-1} \mathbf{H}_{\vec{i}} + \Lambda_f^{-1})^{-1}$. We can also equivalent express the marginal likelihood as below.

$$L(\mathbf{X} | \Theta) \propto -\frac{1}{2} \mathbf{f}_i^\top \left(\Lambda_{\vec{i}}^{-1} - \Lambda_{\vec{i}}^{-1} \mathbf{H}_{\vec{i}} \Sigma_i \mathbf{H}_{\vec{i}}^\top \Lambda_{\vec{i}}^{-1} \right) \mathbf{f}_i - \frac{1}{2} (\log |\Lambda_{\vec{i}}| + \log |\Lambda_f| - \log |\Sigma_i|), \quad (4)$$

We use the form in eq. (4) to derive the updating formulas and criteria for rank selection since it does not involve the inverse of a large non-diagonal matrix.

Model parameters in eq. (3) or eq. (4) are not identifiable due to (1) parameters rescaling from $(\Phi_k, \mathbf{V}_k, \beta_k, s_k^2)$ to $(c_1 \Phi_k, c_2 \mathbf{V}_k, c_3 \beta_k, c_3^2 s_k^2)$ for any $c_1 c_2 c_3 = 1$, and (2) reordering of different component k for $k = 1, \dots, K$. More discussions of the model identifiability can be found in Lock and Li (2018). Hence, adopting similar rules from Lock and Li (2018), we require

$$(C.1) \quad \|\mathbf{V}_k\|_2^2 = 1, \|\Phi_k\|_2^2 = T.$$

$$(C.2) \quad \text{The latent components are in decreasing order based on their overall variances } \Lambda_{f,kk} + \|\mathbf{Z}\beta_k\|_2^2/I, \text{ and the first non-zero entries in } \mathbf{V}_k \text{ and } \Phi_k \text{ to be positive, e.g., } v_{k1} > 0 \text{ and } \phi_{k1} > 0 \text{ if they are non-zero.}$$

To deal with the sparse sampling along the time dimension and take into consideration that features are often smooth over time in practice, we assume that the time component Φ_k is sampled from a slowly varying trajectory function $\phi_k(t)$, and encourage smoothness of $\phi_k(t)$ by directly penalizing the function values via a penalty term $\sum_k \lambda_{1k} \Phi_k^\top \Omega \Phi_k$. This

paper considers a Laplacian smoothing (Sorkine et al., 2004) with a weighted adjacency matrix Γ . Let $\mathcal{T}(t)$ represent the associated time for $\mathbf{X}_{\cdot,t,\cdot}$. We define Ω and Γ as

$$\Omega = \Gamma^\top \Gamma, \quad \Gamma = \begin{pmatrix} \frac{1}{\mathcal{T}[2]-\mathcal{T}[1]} & -\frac{1}{\mathcal{T}[2]-\mathcal{T}[1]} & \cdots & 0 & 0 \\ 0 & \frac{1}{\mathcal{T}[3]-\mathcal{T}[2]} & \ddots & 0 & \vdots \\ \vdots & \vdots & \ddots & \vdots & \vdots \\ 0 & 0 & \cdots & \frac{1}{\mathcal{T}[T]-\mathcal{T}[T-1]} & -\frac{1}{\mathcal{T}[T]-\mathcal{T}[T-1]} \end{pmatrix} \in \mathbb{R}^{T \times (T-1)}$$

Practitioners may choose other forms for Ω . If practitioners want $\phi_k(t)$ to have slowly varying derivatives, they can also use a penalty matrix that penalizes changes in gradients over time.

Further, when the number of covariates q in \mathbf{Z} is moderately large, we may wish to impose sparsity in the $\boldsymbol{\beta}$ parameter. We encourage such sparsity by including a lasso penalty (Tibshirani, 2011) in the model. In summary, our goal is then to find parameters maximizing the expected penalized log-likelihood, or minimizing the penalized expected deviance loss, under norm constraints:

$$\begin{aligned} \min J(\Theta) &:= -\frac{1}{2}L(\mathbf{X}|\Theta) + \sum_{k=1}^K \lambda_{1k} \boldsymbol{\Phi}_k^\top \Omega \boldsymbol{\Phi}_k + \sum_k \lambda_{2k} |\boldsymbol{\beta}_k| \\ \text{s.t. } &\|\mathbf{V}_k\|_2^2 = 1, \|\boldsymbol{\Phi}_k\|_2^2 = T, \text{ for all } k = 1, \dots, K. \end{aligned} \quad (5)$$

Only the identifiability constraint (C.1) has entered the objective. We can always guarantee (C.2) by changing the signs in \mathbf{V} , $\boldsymbol{\Phi}$, $\boldsymbol{\beta}$ and reordering the components afterward without changing the achieved objective value.

Eq. (5) describes a non-convex problem. We will find locally optimal solutions via an alternating update procedure: (1) fixing other parameters and updating $\boldsymbol{\beta}$ via lasso regressions; (2) fixing $\boldsymbol{\beta}$ and updating other model parameters using the EM algorithm. We give details of our iterative estimation procedure in Section 3.

3 Model parameter estimation

Given the model rank K and penalty terms λ_{1k} , λ_{2k} , we alternately update parameters $\boldsymbol{\beta}$, \mathbf{V} , \mathbf{U} , s^2 and σ^2 with a mixed EM procedure described in Algorithm 1. We briefly explain the updating steps here:

(1): Given other parameters, we find β to directly minimize the objective by solving a least-squares regression problem with lasso penalty.

(2): Fixing β , we update the other parameters using an EM procedure. Denote the current parameters as Θ_0 . Our goal is to minimize the penalized expected negative log-likelihood

$$J(\Theta; \Theta_0) := \mathbb{E}_{\mathbf{U}|\Theta_0} \left\{ -L(\mathbf{X}, \mathbf{U}|\Theta) + \sum_k \lambda_{1k} \Phi_k^\top \Omega \Phi_k + \sum_k \lambda_{2k} |\beta_k| \right\}, \quad (6)$$

under the current posterior distribution $\mathbf{U}|\Theta_0$. We adopt a block-wise parameter updating scheme where we update \mathbf{V}_k , Φ_k , Λ_f and σ_j^2 sequentially.

Algorithm 1: SPACO with fixed penalties

Data: \mathbf{X} , Ω , λ_1 , λ_2 , K

Result: Estimated \mathbf{V} , Φ , β , s^2 , σ^2 and posterior $\mathbf{P}(\mathbf{U}|\Theta, \mathbf{X})$ and the marginalized density $\mathbf{P}(\mathbf{X}|\Theta)$.

```

1 Initialization of  $\mathbf{V}$ ,  $\Phi$ ,  $\beta$ ,  $s^2$ ,  $\sigma^2$  and the posterior distribution of  $\mathbf{U}$ ;
2 while Not converged do
3   for  $k = 1, \dots, K$  do
4      $\beta_{:,k} \leftarrow \arg \min_{\beta_{:,k}} \{-L(\mathbf{X}|\Theta) + \lambda_{2k} |\beta_{:,k}| \}$ 
5      $\mathbf{V}_k \leftarrow \arg \min_{\mathbf{V}_k} [J(\Theta; \Theta_0) + \nu \|\mathbf{V}_k\|_2^2]$ ,  $\nu$  is the largest value leading to the
       minimizer having  $\|\mathbf{V}_k\|_2^2 = 1$ 
6      $\Phi_k \leftarrow \arg \min_{\Phi_k} [J(\Theta; \Theta_0) + \nu \|\Phi_k\|_2^2]$ ,  $\nu$  is the largest value leading to the
       minimizer having  $\|\Phi_k\|_2^2 = T$ 
7      $s_k^2 \leftarrow \arg \min_{s_k^2} \mathbb{E}_{\mathbf{U}|\Theta_0} L(\mathbf{X}, \mathbf{U}|\Theta)$ .
8   end
9   For  $j = 1, \dots, J$ :  $\sigma_j^2 \leftarrow \arg \min_{\sigma_j^2} \mathbb{E}_{\mathbf{U}|\Theta_0} L(\mathbf{X}, \mathbf{U}|\Theta)$ .
10  Update the posterior distribution of  $\mathbf{U}$ .
11 end
```

Algorithm 1 describes the high level ideas of our updating schemes. In line 5 and 6, we guarantee the norm constraints on \mathbf{V}_k and Φ_k by adding an additional quadratic term and set the coefficient ν to guarantee the norm requirements. Even though this is not a convex problem, the proposed approaches provide optimal solutions for sub-routines updating different parameter blocks, and the penalized (marginalized) deviance loss is non-

increasing over the iterations.

Theorem 3.1 *In Algorithm 1, let Θ_ℓ and $\Theta_{\ell+1}$ are the estimated parameters at the beginning and end of the ℓ^{th} iteration of the outer **while** loop. We have $J(\Theta^\ell) \geq J(\Theta^{\ell+1})$.*

Proof of Theorem 3.1 is given in Appendix B.1. In Algorithm 1, the posterior distribution of \mathbf{u}_i for each row in \mathbf{U} is Gaussian, with posterior covariance the same as Σ_i defined earlier, and posterior mean given below.

$$\boldsymbol{\mu}_i = \Sigma_i \left(\Lambda_f^{-1} \boldsymbol{\beta}^\top \mathbf{z}_i + (\mathbf{H})_{\vec{i}}^\top \Lambda_{\vec{i}}^{-1} \mathbf{X}_{I, \vec{i}} \right). \quad (7)$$

Explicit formulas and steps for carrying out the subroutines at lines 4-7 and line 9 are deferred to Appendix A.1

4 Initialization, tuning and testing

4.1 Initialization

One initialization approach is to form a Tucker decomposition $[\mathbf{U}_\perp, \boldsymbol{\Phi}_\perp, \mathbf{V}_\perp; \mathbf{G}]$ of \mathbf{X} using HOSVD/MLSVD (De Lathauwer et al., 2000) where $\mathbf{G} \in \mathbb{R}^{K_1 \times K_2 \times K_3}$ is the core tensor and $\mathbf{U}_\perp \in \mathbb{R}^{I \times K_1}$, $\boldsymbol{\Phi}_\perp \in \mathbb{R}^{T \times K_2}$, $\mathbf{V}_\perp \in \mathbb{R}^{J \times K_3}$ are unitary matrices multiplied with the core tensors along the subject, time and feature directions respectively ($K_1/K_2/K_3$ is the smallest between K and $I/T/J$), and then perform PARAFAC decomposition on the small core tensor \mathbf{G} (Bro and Andersson, 1998; Phan et al., 2013). We initialize SPACO with Algorithm 2, which combines the above approach with functional PCA (Yao et al., 2005) to work with sparse longitudinal data. Algorithm 2 consists of the following steps: (1) perform SVD on \mathbf{X}_J to get \mathbf{V}_\perp ; (2) project \mathbf{X}_J onto each column of \mathbf{V}_\perp and perform functional PCA to estimate $\boldsymbol{\Phi}_\perp$; (3) run a ridge-penalized regression of rows of \mathbf{X}_I on $\mathbf{V}_\perp \otimes \boldsymbol{\Phi}_\perp$, and estimate \mathbf{U}_\perp and \mathbf{G} from the regression coefficients

In a noiseless model with $\delta = 0$ and complete temporal observations, one may replace the functional PCA step of Algorithm 2 with standard PCA. Then $[\mathbf{U}, \boldsymbol{\Phi}, \mathbf{V}]$ becomes a PARAFAC decomposition of $\frac{1}{1+\delta} \mathbf{X}$.

Algorithm 2: Initialization of SPACO

- 1 Let \mathbf{V}_\perp be the top K_3 left singular vectors of \mathbf{X}_J using only the observed columns.
 - 2 Set $\mathbf{Y}(k) = (\mathbf{Y}_1(k), \dots, \mathbf{Y}_T(k)) \in \mathbb{R}^{I \times T}$, where $\mathbf{Y}_t(k) = \mathbf{X}_{:,t,:}(\mathbf{V}_\perp)_k \in \mathbb{R}^I$.
 - 3 Let Φ_\perp be the top K_2 eigenvectors from functional PCA on the row aggregation of matrices $\mathbf{Y}(k)$ $k = 1, \dots, K_3$. (see Appendix A.2 for details on functional PCA.)
 - 4 Let $\tilde{\mathbf{U}} = \arg \min_{\mathbf{U}} \{\|\mathbf{X}_I - \mathbf{U}(\mathbf{V}_\perp \otimes \Phi_\perp)^\top\|_F^2 + \delta \|\mathbf{U}\|_F^2\} \in \mathbb{R}^{I \times K^2}$ for some small δ .
 - 5 Let \mathbf{U}_\perp be the top K left singular eigenvectors of $\tilde{\mathbf{U}}$, and $\tilde{\mathbf{G}} = \mathbf{U}_\perp^\top \tilde{\mathbf{U}} \in \mathbb{R}^{K \times K^2}$.
Let $\mathbf{G} \in \mathbb{R}^{K \times K \times K}$ be the estimated core array from rearranging $\tilde{\mathbf{G}}$.
 - 6 Let $\sum_{k=1}^K \mathbf{A}_k \odot \mathbf{B}_k \odot \mathbf{C}_k$ be the rank- K CP approximation of \mathbf{G} . Stack these as the columns of $\mathbf{A}, \mathbf{B}, \mathbf{C} \in \mathbb{R}^{K \times K}$, and set $[\mathbf{U}, \Phi, \mathbf{V}] = [\mathbf{U}_\perp \mathbf{A}, \Phi_\perp \mathbf{B}, \mathbf{V}_\perp \mathbf{C}]$.
 - 7 For each $k = 1, \dots, K$, rescale the initializers to satisfy constraints on \mathbf{V} and Φ .
-

Lemma 4.1 Suppose $\mathbf{X} = \sum_{k=1}^K \mathbf{U}_k^* \odot \Phi_k^* \odot \mathbf{V}_k^*$ and is completely observed. Replace Φ_\perp in Algorithm 2 by the top K eigenvectors of $\mathbf{W} = \frac{1}{I} \sum_{k=1}^K \mathbf{Y}(k)^\top \mathbf{Y}(k)$. Then, the outputs $\mathbf{U}, \Phi, \mathbf{V}$ of Algorithm 2 satisfy that $\mathbf{X} = (1 + \delta) \sum_{k=1}^K \mathbf{U}_k \odot \Phi_k \odot \mathbf{V}_k$.

Proof of Lemma 4.1 is given in Appendix B.2.

4.2 Auto-selection of tuning parameters

Selection of regularizers λ_1 and λ_2 : One way to choose the tuning parameters λ_{1k} and λ_{2k} is to use cross-validation. However, this can be computationally expensive even if we tune each parameter sequentially. It is also difficult to determine a good set of candidate values for the parameters before running SPACO. Instead, we determine the tuning parameters via nested cross-validation, which has been shown to be empirically useful (Huang et al., 2008; Li et al., 2016). In nested cross-validation, the parameters are tuned within their corresponding subroutines:

- (1) In the update for Φ_k , perform column-wise leave-one-out cross-validation to select λ_{1k} , where we leave out all observations from a single time point. (See Appendix A.3.)
- (2) In the update for $\beta_{:,k}$, perform K -fold cross-validation to select λ_{2k} .

Rank selection: We can perform rank selection via cross-validation as suggested in SupCP (Lock and Li, 2018). To reduce the computational cost, we deploy two strategies. (1) Early

stopping: we stop where the cross-validated marginal log-likelihood is no longer decreasing.

(2) Warm start and short-run: we initialize the model parameters for each cross-validated model at the global solution and only run a small number of iterations. We found 5 or 10 iterations are usually sufficiently large in practice (the default maximum number of iterations is 10).

4.3 Covariate importance

In our synthetic experiments in Section 5, we observe that the inclusion of Z can result in a better estimate of the subject scores when the true subject scores strongly depend on Z . A natural following-up question is if we can ascertain the importance of such covariates when they exist. Here, we consider the construction of approximated p-values from conditional independence/marginal independence tests between \mathbf{Z}_j and \mathbf{U}_k :

$$H_{0k}^{partial} : Z_j \perp\!\!\!\perp \mu_k | Z_{j^c}, \quad H_{0k}^{marginal} : Z_j \perp\!\!\!\perp \mu_k$$

Both questions are of practical interest.

Recap on randomization-based hypothesis testing: Before we proceed to our proposal, we review some basic results for hypothesis testing via randomization. Consider a linear regression problem where $Y = Z\beta + \zeta = f(Z) + \zeta$, with mean-zero noise $\zeta \perp\!\!\!\perp Z$. Randomization test is a procedure for constructing a valid p-value without assuming the correctness of the linear model of Y on Z .

Testing for marginal independent between Y and any covariate Z_j is straightforward. Let $t(\mathbf{Z}_j, \mathbf{y})$ be a test statistic. Let $T := t(\mathbf{Z}_j, \mathbf{y})$ and $T^* := t(\mathbf{Z}_j^*, \mathbf{y})$, where \mathbf{Z}_j^* is a permutation of Z_j . Then, under the null hypothesis $H_0^{marginal}$, T are exchangeable with independent copies of T^* . Hence, $P(T > t_{1-\alpha}^* | \mathbf{y}) \leq \alpha$ for any $\alpha \in (0, 1)$ where $t_{1-\alpha}^*$ is the $(1 - \alpha)$ -percentile of the empirical distribution formed by copies T^* and ∞ .

Suppose that we have access to the conditional distribution of $Z_j | Z_{j^c}$. Let $t(\mathbf{Z}_j, \mathbf{Z}_{j^c}, \mathbf{y})$ be a test statistic. Let $T := t(\mathbf{Z}_j, \mathbf{Z}_{j^c}, \mathbf{y})$ and $T^* := t(\mathbf{Z}_j^*, \mathbf{Z}_{j^c}, \mathbf{y})$, where \mathbf{Z}_j^* is an independent copy generated from the conditional distribution $Z_j | Z_{j^c}$ and \mathbf{Z}_{j^c} . Then, under the null hypothesis $H_0^{partial}$, T and T^* have the same law conditional on \mathbf{Z}_{j^c} and \mathbf{y} . So $P(T > t_{1-\alpha}^* | \mathbf{Z}_{j^c}, \mathbf{y}) \leq \alpha$, where $t_{1-\alpha}^*$ is the $(1 - \alpha)$ -percentile of the conditional distribution of T^* (Candès et al., 2018).

Oracle randomization test in SPACO: Let's now go back to SPACO and consider the ideal setting where \mathbf{V} , Φ , s^2 and σ^2 are given. Lemma 4.2 forms the basis of our proposal.

Lemma 4.2 *Given \mathbf{V} , Φ , s^2 , σ^2 , and let β_ℓ^* be the true regression coefficients on the covariates Z for μ_ℓ , $\ell = 1, \dots, K$. For any $k = 1, \dots, K$, we define*

$$\Sigma_i(\delta) = \left(\delta \Lambda_f + (\mathbf{V} \odot \Phi)_{\vec{i}}^\top \Lambda_{\vec{i}} (\mathbf{V} \odot \Phi)_{\vec{i}} \right)^{-1}, \quad (8)$$

$$w_i(\delta) = s_k^2 + (1 - 2\delta) \Sigma_i(\delta)_{kk} + (\delta^2 - \delta) \Sigma_i(\delta)_{k,:} \Lambda_f \Sigma_i(\delta)_{:,k}, \quad (9)$$

$$\tilde{z}_i(\delta) = \left(1 - \delta \frac{\Sigma_i(\delta)_{kk}}{s_k^2} \right) \mathbf{z}_i, \quad \tilde{y}_i(\delta) = \Sigma_i(\delta)_{k,:} (\mathbf{V} \odot \Phi)^\top \Lambda_{\vec{i}} \mathbf{X}_{I,\vec{i}} + \delta \sum_{\ell \neq k} \frac{\Sigma_i(\delta)_{k\ell}}{s_\ell^2} \mathbf{z}_i^\top \beta_\ell. \quad (10)$$

Then, set $\Delta_i(\delta) = \delta \sum_{\ell \neq k} \frac{\Sigma_i(\delta)_{k\ell}}{s_\ell^2} \mathbf{z}_i^\top (\beta_\ell - \beta_\ell^*)$, $\tilde{y}_i(\delta)$ can be expressed as

$$\tilde{y}_i(\delta) = \tilde{\mathbf{z}}_i(\delta)^\top \beta_k^* + \Delta_i(\delta) + \xi_i, \quad \xi_i \sim \mathcal{N}(0, w_i(\delta)). \quad (11)$$

Proof of Lemma 4.2 is given in Appendix B.3. As a result, when the term $\Delta_i(\delta) = 0$, we can apply the traditional randomization tests with response $\tilde{y}_i(\delta)$ and features $\tilde{\mathbf{z}}_i(\delta)$ for subject i . Proposition 4.3 gives our construction of the observed and randomized test statistics .

Proposition 4.3 *Set $T_{\text{partial}}(\delta) = \frac{\sum_i \frac{1}{w_i(\delta)} (\tilde{y}_i(\delta) - \tilde{\mathbf{z}}_{i,j^c}^\top(\delta) \beta_{j^c,k}) \tilde{z}_{ij}(\delta)}{\sum_i \frac{1}{w_i(\delta)} \tilde{z}_{ij}^2(\delta)}$, $T_{\text{marginal}}(\delta) = \frac{\sum_i \frac{1}{w_i(\delta)} \tilde{y}_i(\delta) \tilde{z}_{ij}(\delta)}{\sum_i \frac{1}{w_i(\delta)} \tilde{z}_{ij}^2(\delta)}$.*

Replacing Z_j with the properly randomized Z_j^ to create $T_{\text{marginal}}^*(\delta)$ and $T_{\text{partial}}^*(\delta)$ (Z_j^* is the permutation of Z_j in $T_{\text{marginal}}^*(\delta)$ and is independently generated from $Z_j | \mathbf{Z}_{j^c}$ in $T_{\text{partial}}^*(\delta)$).*

When $\Delta(\delta) = 0$, we have

$$T_{\text{marginal}}(\delta) | \tilde{\mathbf{y}}(\delta) \stackrel{d}{=} T_{\text{marginal}}^*(\delta) | \tilde{\mathbf{y}}(\delta), \quad \text{under } H_{0k}^{\text{marginal}}, \quad (12)$$

$$T_{\text{partial}}(\delta) | (\tilde{\mathbf{y}}(\delta), \mathbf{Z}_{j^c}) \stackrel{d}{=} T_{\text{partial}}^*(\delta) | (\tilde{\mathbf{y}}(\delta), \mathbf{Z}_{j^c}), \quad \text{under } H_{0k}^{\text{partial}}. \quad (13)$$

In practice, β_ℓ for the other factors $\ell \neq k$ are also estimated from the data. When $\delta \neq 0$, we could have $\Delta_i(\delta) \neq 0$, which renders the randomization test invalid. Thus, we typically set $\delta = 0$. For convenience, we drop the δ argument when $\delta = 0$, e.g., $T_{\text{partial}} = T_{\text{partial}}(\delta)$. Algorithm 3 summarizes our proposal.

Remark 4.3.1 *For $\delta > 0$, the test based on $\tilde{y}_i(\delta)$, $w(\delta)$, and $\tilde{\mathbf{z}}_i(\delta)$ trades off robustness against estimation errors in $Z^\top (\beta_\ell - \beta_\ell^*)$ for possibly increased power. To see this, suppose*

Algorithm 3: Randomization test for \mathbf{Z}_j

```

1 for  $k = 1, \dots, K$  do
3   Construct responses and features as described in Lemma 4.2, for  $\delta = 0$ .
5   Define  $\hat{\beta}_k$  by
      
$$\hat{\beta}_k = \arg \min_{\beta_k: \beta_{k,j}=0} \left\{ \sum_{i=1}^I \frac{1}{w_i(0)} (\mathbf{z}_i^\top \beta_k - \tilde{y}_i(0))^2 + \lambda_{2k} |\beta_k|_1 \right\}.$$

7   Compute the designed test statistic  $T$  using  $(\mathbf{Z}_j, \mathbf{Z}_{j^c}, \tilde{\mathbf{y}}(0), \hat{\beta}_{j^c,k})$ .
9   Compute randomized statistics  $T_b^*$  using  $(\mathbf{Z}_j^{b*}, \mathbf{Z}_{j^c}, \tilde{\mathbf{y}}(0), \hat{\beta}_{j^c,k})$ , where  $\mathbf{Z}_j^{b*}$  for
       $b = 1, \dots, B$  are (conditionally or marginally) independent copies of  $\mathbf{Z}_j$ .
11  Let  $\hat{G}(\cdot)$  be the empirical estimate of the CDF of  $T$  under  $H_0$  using
       $\{T_1^*, \dots, T_B^*\}$ , and return the two-sided p-value  $p = [1 - \hat{G}(|T|)] + \hat{G}(-|T|)$ .
12 end

```

that $\beta_\ell = \beta_\ell^*$ for $\ell \neq k$ and $Z_j \sim \mathcal{N}(0, 1)$. The signal to noise ratio with $\delta \in \{0, 1\}$ can be calculated as

$$\text{SNR}(0) = \frac{\mathbb{E}(\mathbf{z}_i^\top \beta_k^*)^2}{\frac{1}{I} \sum_i w_i(0)} = \frac{\|\beta_k^*\|_2^2}{s_k^2 + \frac{1}{I} \sum_i \Sigma_i(0)_{kk}}, \text{SNR}(1) = \frac{\frac{1}{I} \sum_i \mathbb{E}(\tilde{\mathbf{z}}_i(1)^\top \beta_k^*)^2}{\frac{1}{I} \sum_i w_i(1)} = \frac{\|\beta_k^*\|_2^2}{s_k^2}.$$

Thus, the signal-to-noise ratio is higher with $\delta = 1$ if we have access to the true β_ℓ^* .

The conditional randomization test requires generating Z_j^* from the conditional distribution $Z_j|Z_{j^c}$. We estimate the conditional distribution of Z_j^* via proper exponential family distribution. More details on the generations of \mathbf{Z}_j^* are provided in Appendix A.4.

Approximated p-value construction with estimated model paramters: The true model parameters for \mathbf{V} , Φ , s^2 and σ^2 are of course unknown. We will substitute their empirical estimates in the above procedure. However, the substitutes from a full SPACO fit may suffer from fitting towards the empirical noise. To reduce the influence of over-fitting, we use \mathbf{V}, Φ from cross-validation as described for performing the rank selection. That is, for $i \in \mathcal{V}_m$ where \mathcal{V}_m is the index set for fold m in cross-validation, we construct $\tilde{y}_i(0) = \Sigma_i(0)_{k,:}(\mathbf{V}^{-m} \odot \Phi^{-m})^\top \Lambda_{\vec{i}} \mathbf{X}_{I,\vec{i}}$, where \mathbf{V}^{-m} , Φ^{-m} are estimates using fold other than \mathcal{V}_m . $\Sigma_i(0)$ is also estimated using \mathbf{V}^{-m} , Φ^{-m} and cross-validated prior covariance

Λ_f^{-m} . We refer it as cross-fit, where we estimate some model parameters using data from other folds and update the quantity of interest using them and the current fold. Since each fold is initialized at the global solution, this further encourages the comparability of the constructed \tilde{y} and \tilde{z} from different folds. We observe that the cross-fit offers better Type I error control than the naive plug-in of the full estimates.

5 Numerical studies with synthetic data

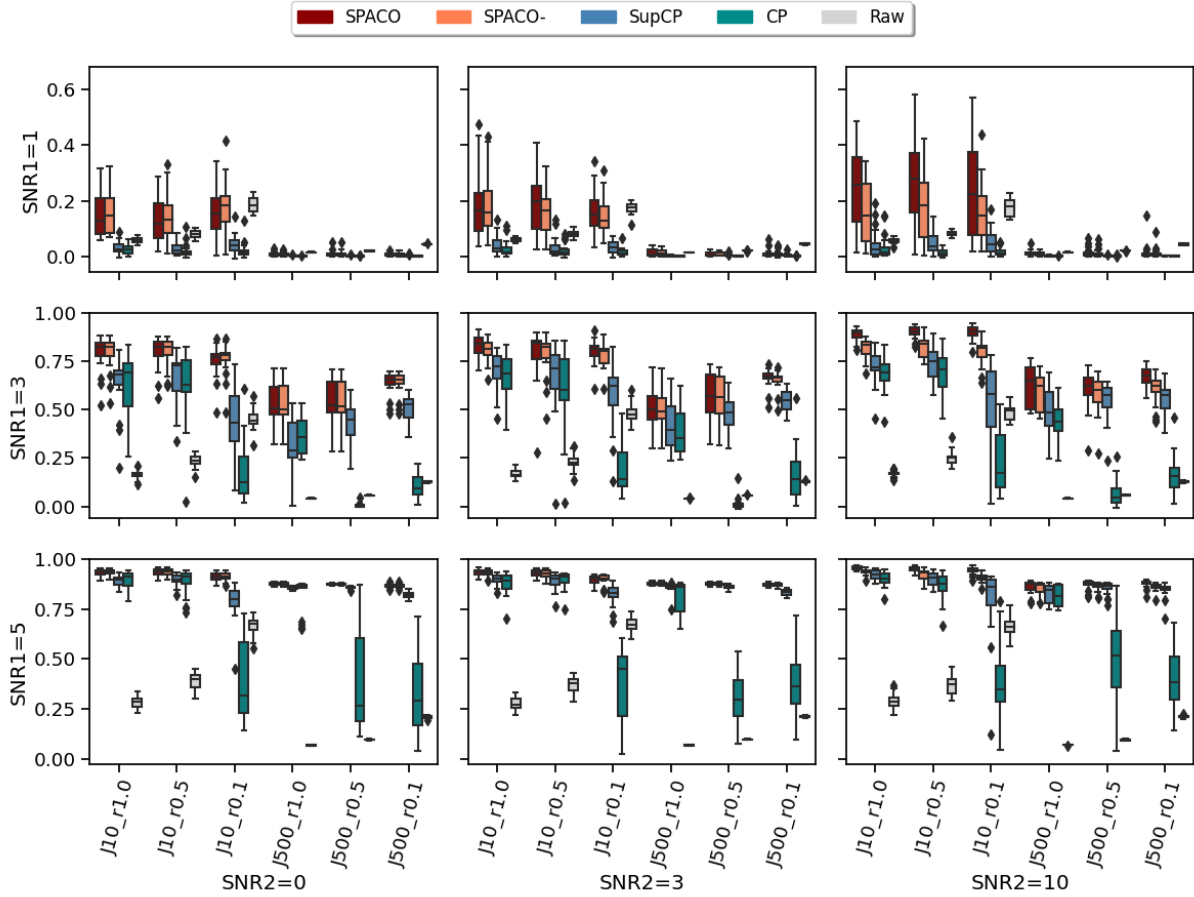
In this section, we evaluate SPACO with synthetic Gaussian data. We fix the variance at 1 for the noise ϵ and the number of true ranks $K = 3$. We consider simulated data (\mathbf{X}, \mathbf{Z}) with dimensions $(I, T, J, q) = (100, 30, 10, 100)$ and $(100, 30, 500, 100)$, with the observed rate ($= 1 - \text{missing rate}$) along the time dimension $r \in \{100\%, 50\%, 10\%\}$ and observed time stamps chosen randomly for each subject. Given the dimension and the observed rate, we generate $v_{jk} \stackrel{i.i.d.}{\sim} \mathcal{N}(0, \frac{1}{j})$ and $z_{i\ell} \stackrel{i.i.d.}{\sim} \mathcal{N}(0, 1)$ for $i = 1, \dots, I$, $j = 1, \dots, J$ and $\ell = 1, \dots, q$. Then, (1) we set $\phi_1(t) = \theta_1$, $\phi_2(t) = \theta_2 \sqrt{1 - (\frac{t}{T})^2}$, $\phi_3(t) = \theta_3 \cos(4\pi \frac{t}{T})$ with random parameters $\theta_1, \theta_2, \theta_3 \sim c_1 \cdot \mathcal{N}(0, \frac{\log J + \log T}{nT\gamma})$ for $c_1 \in \{1, 3, 5\}$, and (2) we set $\beta_{\ell,k} \sim c_2 \cdot \mathcal{N}(0, \frac{\log q}{I})$ for $c_2 \in \{0, 3, 10\}$ for the first $\ell = 1, 2, 3$, and set $\beta_{\ell,k} = 0$ otherwise. Each \mathbf{U}_k is standardized to be mean 0 and variance 1 after generation. This generates 54 different simulation setups in total.

5.1 Reconstruction quality evaluation

We compare SPACO, SPACO-, plain CP from python package *tensorly*, and a proxy to SupCP by setting $\lambda_{1k} = \lambda_{2k} = 10^{-2}$ as small fixed values in SPACO (the additional small penalties improve numerical stability to deal with large q and high missing rate). Although this is not exactly SupCP, they are very similar. We refer to this special case of SPACO as SupCP and include it to evaluate the gain from smoothness regularization on the time trajectory. Note that we use the proposed initialization in SPACO, SPACO- and SupCP, which provide better and more stable results when the missing rate is high. A comparison between SupCP with random and proposed initialization is given in Appendix C.1. We use the true rank in all four methods in our estimation. Figure 1 shows the achieved correlation between the reconstructed tensors and the underlying signal tensors across different setups and 20 random repetitions. SNR1 represents c_1 , SNR2 represents c_2 , and

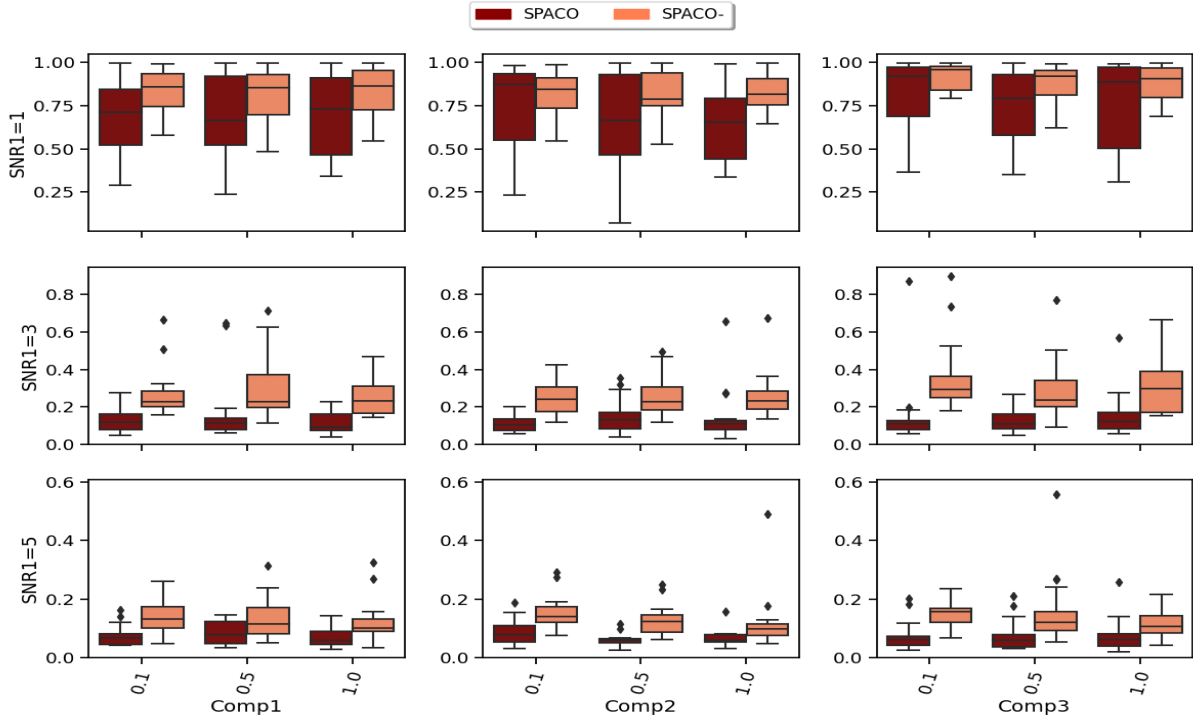
each sub-plot represents different signal-to-noise ratios SNR1 and SNR2, as indicated by its row and column names. The y and x axes indicate the achieved correlation and different combinations of J and observed rate, respectively. For example, x-axis label $J10_r0.1$ means the feature dimension is 10, and 10% of entries are observed. The “Raw” method indicates the results by correlating the true signal and the empirical observation on only the observed entries. It is not directly comparable to others with missing data, but we include it here to show the signal level of different simulation setups. We also compare the reconstruction quality on missing entries in Appendix C.2.

Figure 1: Reconstruction evaluation by the correlations between the estimates and the true signal tensor. In each subplot, x axis label indicates different J and observing rate, the y axis is the achieved correlation, and the box colors represent different methods. The corresponding subplot column/row name represents the signal-to-noise ratio SNR1/SNR2.



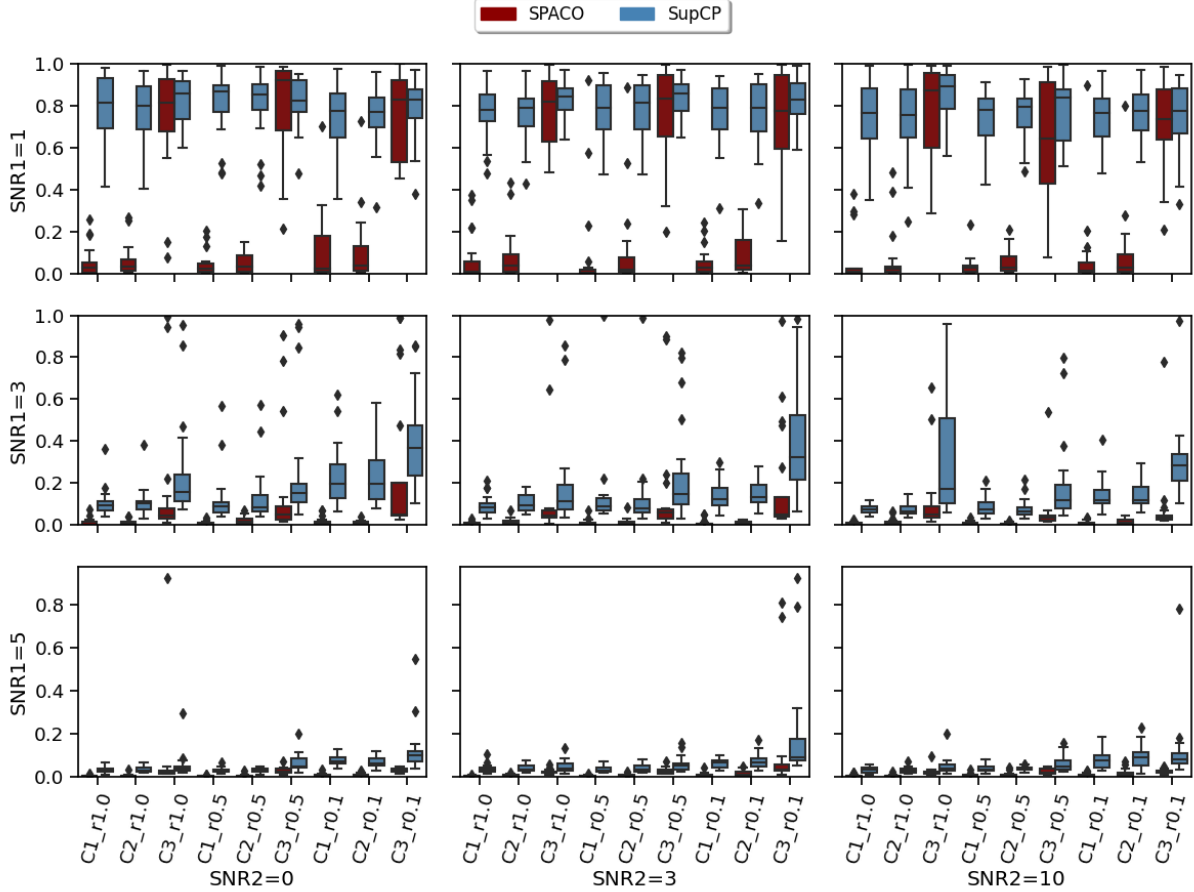
SPACO outperforms SPACO- when the subject score U depends strongly on Z , which could result from a more accurate estimation of the subject scores. To confirm this, we evaluate the estimation quality of U at $J = 10$ and $\text{SNR2} = 10$ and measure the estimation quality by R^2 (regressing the true subject scores on the estimated ones). In Figure 2, we shows the achieved $(1 - R^2)$ for SPACO and SPACO- (smaller is better), where x-axis label represents the observing rate and column names represent the component, e.g., $\text{Comp1} \rightarrow U_1$.

Figure 2: Comparison of SPACO and SPACO- for reconstructing U at $J = 10$, $\text{SNR2} = 10$. In each subplot, x axis label indicates different component and observing rate, the y axis is the achieved $(1 - R^2)$, and the box colors represent different methods. The corresponding subplot column/row name represents the signal-to-noise ratio SNR1 /component.



SPACO /SPACO- are both top performers for our smooth tensor decomposition problem and achieve significantly better performance than CP and SupCP when the signal is weak and when the missing rate is high by utilizing the smoothness of the time trajectory. To see this, we compared the estimation quality of the time trajectories using SPACO and SupCP. In Figure 3, we shows the achieved $(1 - R^2)$ for SPACO and SupCP at $J = 10$. In the x-axis

Figure 3: Comparison of SPACO and SupCP for reconstructing Φ at $J = 10$. In each subplot, x axis label indicates different component and observing rate, the y axis is the achieved $(1 - R^2)$, and the box colors represent different methods. The corresponding subplot column/row name represents the signal-to-noise ratio SNR1/SNR2.



label represents different trajectory and observed rate, e.g., $(C1_r1.0 \rightarrow \text{estimation of } \phi_1(t) \text{ at observing rate } r = 1.0)$. When the signal is weak (SNR1=1), SPACO could approximate the constant trajectory component ($C1$) and start to estimate other trajectories successfully as the signal increases. SPACO achieves significantly better estimation of the true underlying trajectories than SupCP for various signal-to-noise ratios.

5.2 Variable importance and hypothesis testing

We investigate the approximated p-values based on cross-fit for testing the partial and marginal associations of \mathbf{Z} with $\boldsymbol{\eta}$ under the same simulation set-ups. Since our variables

in \mathbf{Z} are generated independently, the two null hypotheses coincide in this setting. However, the two tests have different powers given the same p-value cut-off because the test statistics differ.

The proposed randomization tests for SPACO achieve reasonable Type I error controls. Cross-fit is important for a good Type I error control: In Appendix C.4, we present qq-plots comparing p-values using cross-fitted \mathbf{V} and $\mathbf{\Phi}$ and the naive construction. We observe noticeable deviations from the uniform distribution for the later construction when the signal-to-noise ratio is low. Fig.10 and Fig.5 show the the achieved Type I error and power with p-value cut-offs at $\alpha = 0.01, 0.05$ and with observed rate $r = 0.5$. The type I errors are also well controlled for $r \in \{1.0, 0.1\}$ (Appendix C.3).

Figure 4: Achieved type I errors at observing rate $r = 0.5$. In each subplot, x axis label indicates different combination of feature dimension J and targeted level $\alpha \in \{0.01, 0.05\}$, the y axis is the achieved type I errors. Different bar colors represent different tests (partial or marginal). The two dashed horizontal lines indicate levels 0.01 and 0.05.

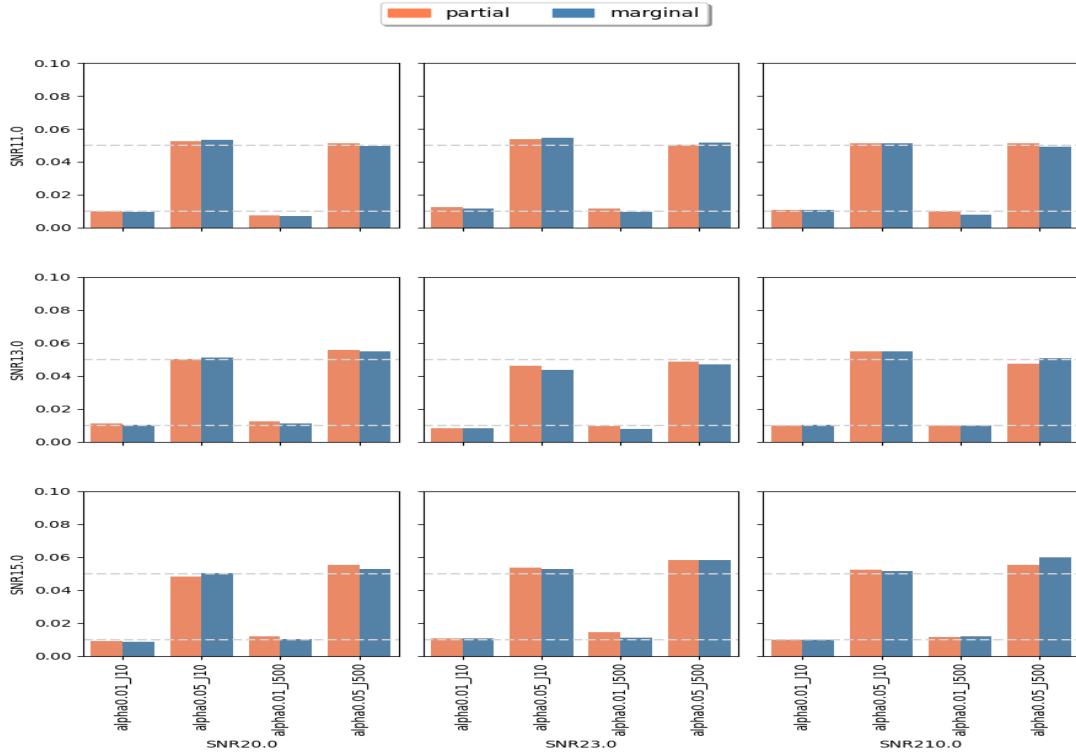
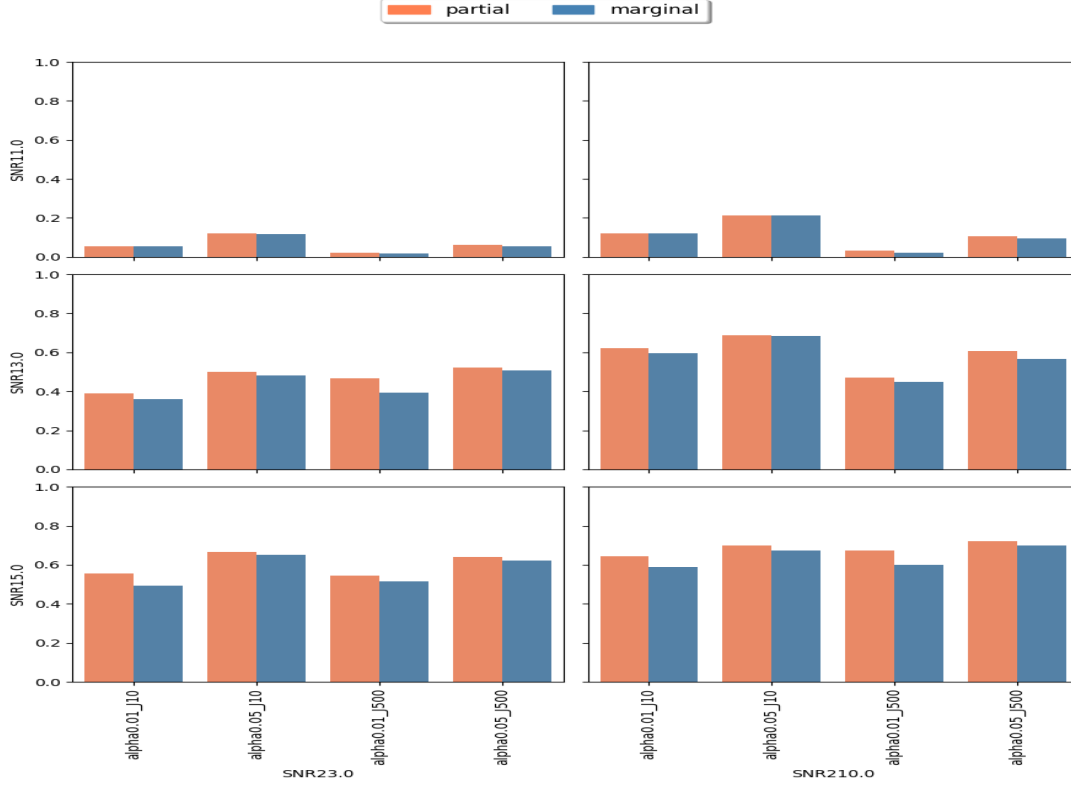


Figure 5: Achieved power at observing rate $r = 0.5$. In each subplot, x axis label indicates different combination of feature dimension J and targeted level $\alpha \in \{0.01, 0.05\}$, the y axis is the achieved power. Different bar colors represent different tests (partial or marginal).

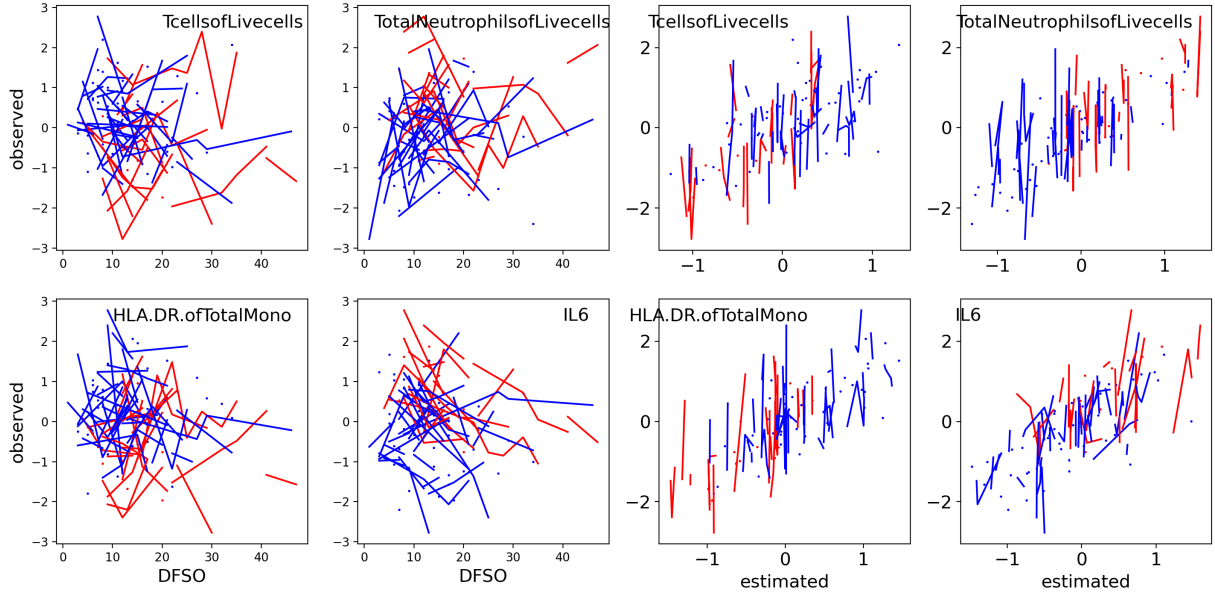


6 Case study

We now apply SPACO to a longitudinal immunological data set on COVID 19 from the IMPACT study (Lucas et al., 2020). Initially, the data contained 180 samples on 135 immunological features, collected from 98 participants with COVID-19 infection. We filter out features with more than 20% missingness among collected samples and imputed the missing observations using MOFA (Argelaguet et al., 2018) for the remaining features. This leaves us with a complete matrix with 111 features and 180 samples, which is organized into a tensor of size $(I, T, J) = (98, 35, 111)$ where T is the number of unique DFSO (days from symptom onsite) in this data set. This is a sparsely observed tensor, and the average observing rate is 1.84 along the time dimension. Apart from the immunological data, the

data set also provides non-immunological covariates. We use eight static risk factors as our covariate \mathbf{Z} (COVID_risk1 - COVID_risk5, age, sex, BMI), and four symptom measures as additional responses (ICU, Clinical score, LengthofStay, Coagulopathy).

Figure 6: Left panel shows examples of time trajectories of four features for different subjects (horizontal time axis is the DFSO) ; right panel shows plots of observed feature values against estimated ones from SPACO. Each line/dot represents observations from a single subject. Subjects in ICU are colored red.



We run SPACO with processed \mathbf{X} , \mathbf{Z} , and model rank $K = 4$, selected from finding the first maxima for the five-fold cross-validated marginal log-likelihood. Fig.6 shows example plots of raw observations against our reconstructions across all samples. We see a positive correlation between these observed and reconstructed values.

Combining static covariates \mathbf{Z} with the longitudinal measurements can sometimes improve the estimation quality of subject scores compared to SPACO-, as we have illustrated in our synthetic data examples. We can not possibly get the true subject scores in the real data set. However, we could still compare the estimated subject scores are clinically relevant by comparing them to the responses. Here, we also run SPACO- with $K = 4$ and

Table 1: Association between estimated subject scores and four response variables. C1-C4 represent the four components in SPACO/SPACO-. C*cor represents the achieved spearman correlation and C*pval is the p-value for the corresponding correlation test.

		C1cor	C1pval	C2cor	C2pval	C3cor	C3pval	C4cor	C4pval
SPACO	ICU	-0.20	4.9E-02	0.37	1.7E-04	0.28	5.4E-03	0.00	9.8E-01
	Clinicalscore	-0.32	1.2E-03	0.42	1.3E-05	0.44	6.4E-06	0.07	4.8E-01
	LengthofStay	-0.10	3.4E-01	0.28	5.2E-03	0.14	1.8E-01	0.11	2.9E-01
	Coagulopathy	-0.03	7.7E-01	0.22	3.1E-02	0.21	3.5E-02	0.03	7.9E-01
SPACO-	ICU	-0.20	5.1E-02	0.38	1.4E-04	0.25	1.5E-02	-0.00	9.6E-01
	Clinicalscore	-0.32	1.3E-03	0.43	1.0E-05	0.40	4.5E-05	0.07	4.9E-01
	LengthofStay	-0.09	3.9E-01	0.29	4.4E-03	0.10	3.5E-01	0.10	3.3E-01
	Coagulopathy	-0.03	8.0E-01	0.22	3.0E-02	0.19	5.9E-02	0.02	8.2E-01

examine if the resulting subject scores from SPACO associate better with the responses. Table 1 shows the spearman correlations and their p-values when comparing the estimated subject scores and each response. The top three components C1, C2, C3 are significantly associated with the responses. Among them, C_2 uniquely captures variability for the length of stay (in hospital), and only C_3 heavily depends on \mathbf{Z} (the estimated coefficients are 0 for both C_1 and C_2). C_3 from SPACO achieved a better association with the clinical outcomes than SPACO. Using the randomization test, we can also test for the contribution of each Z_j to C_3 . Table 2 shows the p-value and adjusted p-value from the partial dependence test and marginal dependence test, with the number of randomization $B = 2000$. The top associate is COVIDRISK_3 (hypertension) with a p-value around 0.01 (adjusted p-value around 0.1). BMI is also weakly associated with C_3 , with p values < 0.05 for both tests. In this data set, we observe that the immunological measurements contain information strongly related to clinical responses of interest. Although some risk factors like hypertension and BMI contains relatively weaker signal, they may still improve the estimated subject scores like in the case of C_3 .

Table 2: Results from randomization test for component 3 (C3). The column nonzero counts the number of 1 for binary covariate COVIDRISK_1 - COVIDRISK_5 and sex (1 = Male, 0 = Female). The adjusted pvalues (pval*) are based on BH correction.

	pval(partial)	pval(marginal)	padj(partial)	padj(marginal)	nonzero
COVIDRISK_1	0.877	0.905	1.000	0.905	7
COVIDRISK_2	0.263	0.063	0.701	0.169	24
COVIDRISK_3	0.013	0.011	0.101	0.088	50
COVIDRISK_4	0.563	0.712	1.000	1.000	23
COVIDRISK_5	0.919	0.885	0.919	1.000	5
Age	0.584	0.423	0.935	0.846	—
sex	0.715	0.727	0.953	0.970	47
BMI	0.029	0.041	0.117	0.166	—

7 Discussion

We propose SPACO to model sparse multivariate longitudinal data and auxiliary covariates jointly. The smoothness regularization may lead to a dramatic improvement in the estimation quality with high missing rates, and access to informative auxiliary covariates could improve the estimation of subject scores. We applied the proposed pipeline to COVID-19 data sets. Even though both data sets are highly sparse and of small size, SPACO identifies components whose subject scores are strongly associated with clinical outcomes of interest and identify static covariates that might contribute to the severe symptoms. A future direction is to extend SPACO to model multi-omics data. Different omics can be measured at different times and have distinct data types or scales. These motivate a tailored model’s more careful design rather than a naive approach of blindly pooling all omics data together.

SUPPLEMENTARY MATERIAL

Python package for SPACO: <https://github.com/LeyingGuan/SPACO>

Python pipeline for reproducing results in the manuscript: <https://github.com/LeyingGuan/SPACOexperments>

A Additional Algorithmic Details

A.1 Updating rules in Algorithm 1

Lemma A.1 provides exact parameter update rules used in Algorithm 1. We also define $\langle \cdot \rangle$ as the expectation of some quantity with respect to the posterior distribution of \mathbf{U} . Let $O \in \{0, 1\}^{I \times T}$ with $O_{it} = 1$ if time t is observed for subject i and $O_{it} = 0$ otherwise.

Lemma A.1 *The parameter update steps in Algorithm 1 take the following forms:*

- In line 4, $\beta_k = \arg \max_{\beta_k} \{L(\mathbf{X}|\Theta) + \lambda_{2k}|\beta_{\cdot k}|\} = \arg \min_{\beta_k} \frac{1}{2}\|\tilde{\mathbf{y}} - \tilde{\mathbf{Z}}\beta_k\|_2^2 + \lambda_{2k}|\beta_k|$, where

$$\tilde{\mathbf{z}}_i = \sqrt{\frac{1}{s_k^2} \frac{s_k^2 - (\Sigma_i)_{k,k}}{s_k^2}} \mathbf{z}_i, \quad (14)$$

$$\tilde{y}_i = \sqrt{\frac{1}{s_k^2} \frac{s_k^2 - (\Sigma_i)_{k,k}}{s_k^2}} \left((\Sigma_i)_{k,:} (\mathbf{V} \odot \Phi)_{\vec{i}}^\top \Lambda_{\vec{i}} \mathbf{X}_{I,\vec{i}} + \sum_{l \neq k} (\Sigma_i)_{k,l} / s_l^2 (\mathbf{z}_i^\top \beta_l) \right). \quad (15)$$

Here $(\Sigma_i)_{k,:}$ is the k^{th} row of Σ_i , and $(\Sigma_i)_{k,\bar{k}}$ is this row with k^{th} entry removed; $\Lambda_{f,\bar{k}}$ is the sub matrix of Λ_f with the k^{th} column and row removed.

- Set $Q_1 = \langle \mathbf{U} \rangle \odot \mathbf{V} \in \mathbb{R}^{IJ \times K}$, $Q_2 \in \mathbb{R}^{K \times J}$ and $Q_3 \in \mathbb{R}^{K \times K \times J}$ with $Q_{2kj} = \frac{1}{\sigma_j^2} \mathbf{X}_{Jj\vec{j}}^\top Q_{1\vec{j}k}$ and $Q_{3k_1k_2j} = \frac{1}{\sigma_j^2} \sum_t \phi_{tk_1} \phi_{tk_2} \sum_{O_{it}=1} (\Sigma_{ik_1k_2} + \langle u_{ik_1} \rangle \langle u_{ik_2} \rangle)$. In line 5, the update of \mathbf{V}_k considers the following problem:

$$\mathbf{V}_k \leftarrow \arg \min_{\mathbf{V}_k} \left[\sum_{j=1}^J \frac{1}{2} (a_{jk} v_{jk}^2 - 2b_{jk} v_{jk}) + \nu \|\mathbf{V}_k\|_2^2 \right],$$

where $a_{jk} = \frac{1}{\sigma_j^2} \|Q_{1,\vec{j},k}\|_2^2 + Q_{3kk,j}$, $b_{jk} = Q_{2kj} - \sum_{k' \neq k} Q_{3kk',j} v_{jk'}$ and ν is the largest value such that the solution satisfies $\|\mathbf{V}_k\|_2^2 = 1$.

- Set $Q_1 = \langle \mathbf{U} \rangle \odot \Phi \in \mathbb{R}^{IT \times K}$, $Q_2 \in \mathbb{R}^{K \times T}$ and $Q_3 \in \mathbb{R}^{K \times K \times T}$ with $Q_{2kt} = \mathbf{X}_{Tt}^\top \text{diag}\{\frac{1}{\sigma_t^2}\} Q_{1t\vec{k}}$ and $Q_{3k_1k_2t} = \sum_j \frac{1}{\sigma_j^2} v_{jk_1} v_{jk_2} \sum_{i:O_{it}=1} (\Sigma_{ik_1k_2} + \langle u_{ik_1} \rangle \langle u_{ik_2} \rangle)$. In line 5, the update of \mathbf{V}_k considers the following problem:

$$\Phi_k \leftarrow \arg \min_{\Phi_k} \left[\sum_{t=1}^T \frac{1}{2} (a_{jk} v_{jk}^2 - 2b_{jk} v_{jk}) + \lambda_{1k} \phi_k^\top \Omega \phi_k + \nu \|\Phi_k\|_2^2 \right],$$

where $a_{tk} = \left(\|\text{diag}\{\frac{1}{\sigma_t}\} Q_{1,\vec{t},k}\|_2^2 + Q_{3kk,t} \right)$, $b_{jk} = \left(Q_{2kt} - \sum_{k' \neq k} Q_{3kk',t} \phi_{tk'} \right)$ and ν is the largest value such that the solution satisfies $\|\Phi_k\|_2^2 = T$.

- In lines 14 and 15,

$$s_k^2 \leftarrow \frac{1}{I} \sum_i [(\mu_{ik} - \mathbf{z}_i^\top \beta_k)^2 + (\Sigma_i)_{kk}],$$

and

$$\sigma_j^2 \leftarrow \frac{1}{|\vec{j}|} \left[(X_{J,\vec{j}} - (\Phi \odot \mu)_{\vec{j}} \mathbf{v}_j)^\top (X_{J,\vec{j}} - (\Phi \odot \mu)_{\vec{j}} \mathbf{v}_j) + \mathbf{v}_j^\top \left(\sum_t \left(\sum_{i:O_{it}=1} \Sigma_i \right) \cdot (\phi_t \phi_t^\top) \right) \mathbf{v}_j \right].$$

Derivation of Lemma A.1 is given in Appendix B.4.

A.2 Functional PCA for initializations

In Yao et al. (2005), the authors suggest a functional PCA analysis by performing eigenvalue decomposition of the smoothed matrix fitted with a local linear surface smoother. Here, we apply the suggested estimation approach on the total product matrix: Let $\hat{\mathbf{W}}_{i,s,t} = \sum_k \mathbf{Y}_{is}(k) \mathbf{Y}_{it}(k)$ be the empirical estimate of the total product matrix for subject i , we first estimate $\mathbb{E}[\hat{W}_{i,s,t}]$ via local surface smoother and then perform PCA on the estimated $\mathbb{E}[\hat{W}_{i,s,t}]$:

- To fit a local linear surface smoother for the off-diagonal element of \mathbf{W}_{s_0,t_0} , we consider the following problem:

$$\min \sum_i \sum_{O_{it} O_{is}=1, s \neq t} \kappa\left(\frac{s-s_0}{h_G}, \frac{t-t_0}{h_G}\right) (\hat{\mathbf{W}}_{i,s,t} - g((s_0, t_0), (s, t), \beta))^2,$$

with $g((s_0, t_0), (s, t), \beta) = \beta_0 + \beta_1(s - s_0) + \beta_2(t - t_0)$, and $\kappa : \mathbb{R}^2 \mapsto \mathbb{R}$ is a standard two-dimensional Gaussian kernel.

- For the diagonal element, we estimate it by local linear regression: for each t_0 :

$$\min \sum_i \sum_{O_{it}=1} \kappa_1\left(\frac{t-t_0}{h_G}\right) (\hat{\mathbf{W}}_{i,t,t} - g(t_0, t, \beta))^2.$$

where $g(t_0, t, \beta) = \beta_0 + \beta_1(t - t_0)$.

By default, we let $h_G = \frac{T}{\sqrt{1 + \sum_{s \neq t} \mathbb{1}\{\sum_i O_{is} O_{it} > 0\}}}$.

A.3 Parameter tuning on λ_{1k}

In this section, we provide more details on the leave-one-time-out cross-validation for tuning λ_{1k} , $\forall k = 1, \dots, K$. From eq. (19), the expected penalized deviance loss can be written as (keeping only terms relevant to Φ):

$$L = \sum_{t=1}^T \left\{ \phi_t^\top \left[(\mathbf{V} \odot \boldsymbol{\mu})_{\vec{t}}^\top \Lambda_{\vec{t}}^{-1} (\mathbf{V} \odot \boldsymbol{\mu})_{\vec{t}} + \sum_j \frac{(\sum_{O_{it}=1} \Sigma_i) \cdot (\mathbf{v}_j \mathbf{v}_j^\top)}{\sigma_j^2} \right] \phi_t - 2\phi_t^\top \left[(\mathbf{V} \odot \boldsymbol{\mu})_{\vec{t}}^\top \Lambda_{\vec{t}}^{-1} \right] \mathbf{X}_{T,\vec{t}} \right\} + \sum_k \lambda_{1k} \Phi_k^\top \Omega \Phi_k.$$

For a given k , we define the diagonal matrix $\mathbf{A} \in \mathbb{R}^{T \times T}$ and the vector $a \in \mathbb{R}^T$ as

$$\mathbf{A}_{tt} = \left[(\mathbf{V} \odot \boldsymbol{\mu})_{\vec{t}}^\top \Lambda_{\vec{t}}^{-1} (\mathbf{V} \odot \boldsymbol{\mu})_{\vec{t}} + \sum_j \frac{(\sum_{O_{it}=1} \Sigma_i) \cdot (\mathbf{v}_j \mathbf{v}_j^\top)}{\sigma_j^2} \right]_{kk}$$

$$a_t = (\mathbf{V}_k \otimes \boldsymbol{\mu}_{\cdot k})_{\vec{t}}^\top \Lambda_{\vec{t}}^{-1} \mathbf{X}_{T,\vec{t}} - \left[(\mathbf{V} \odot \boldsymbol{\mu})_{\vec{t}}^\top \Lambda_{\vec{t}}^{-1} (\mathbf{V} \odot \boldsymbol{\mu})_{\vec{t}} + \sum_j \frac{(\sum_{O_{it}=1} \Sigma_i) \cdot (\mathbf{v}_j \mathbf{v}_j^\top)}{\sigma_j^2} \right]_{k,\bar{k}}^\top \phi_{t,\bar{k}}.$$

When we leave out a specific time point t_0 , we optimize for Φ_k minimizing the following leave-one-out constrained loss,

$$\min_{\Phi_k} J(t_0, k) = \Phi_k^\top (\mathbf{A}(t_0) + \lambda_{1k} \Omega) \Phi_k - 2a(t_0)^\top \Phi_k, \quad \|\Phi_k\|_2^2 = T.$$

We set $\mathbf{A}(t_0)$ as \mathbf{A} with the (t_0, t_0) -entry zeroed out, and $a(t_0)$ as a with $a(t_0)$ zeroed out. The leave-one-time cross-validation error is calculated based on the expected deviance loss (unpenalized) at the leave-out time point t_0 :

$$J_{loocv}(t_0, k) = \mathbf{A}_{t_0, t_0} \left(\hat{\phi}_{t_0 k}^{-t_0} - \frac{a_{t_0}}{\mathbf{A}_{t_0, t_0}} \right)^2,$$

where $\hat{\phi}_{t_0 k}^{-t_0}$ is the leave-one-out estimate. To reduce the computational cost, we drop the norm constraint when picking λ_{1k} , which enables us to adopt the following short-cut:

$$\sum_{t_0} J_{loocv}(t_0, k) = \sum_{t_0} \frac{\mathbf{A}_{t_0, t_0} \left(\hat{\phi}_{t_0 k}^{-t_0} - \frac{a_{t_0}}{\mathbf{A}_{t_0, t_0}} \right)^2}{(1 - [(\mathbf{A} + \lambda_{1k} \Omega)^{-1}]_{t_0 t_0})^2}, \quad (16)$$

where $\hat{\Phi}_k$ is the unconstrained solution from using all time points. This follows from the arguments below:

1. Drop the constraint, the original problem is equivalent to:

$$\min \|(\mathbf{A}(t_0) + \lambda_{1k}\Omega)^{\frac{1}{2}}\Phi_k - (\mathbf{A}(t_0) + \lambda_{1k}\Omega)^{-\frac{1}{2}}a(t_0)\|_2^2$$

2. Consider the augmented problem:

$$\min \|(\mathbf{A} + \lambda_{1k}\Omega)^{\frac{1}{2}}\Phi_k - (\mathbf{A} + \lambda_{1k}\Omega)^{-\frac{1}{2}}\tilde{a}(t_0)\|_2^2$$

where $\tilde{a}(t_0) = a(t_0) + \delta(t_0)$, and $\delta_{t_0}(t_0) = A_{t_0,t_0}\hat{\phi}_{t_0k}^{-t_0}$ and $\delta_t(t_0) = 0$ for $t \neq t_0$. The augmented problem also has $\hat{\Phi}_k^{-t_0}$ as its solution.

3. Hence, without the constraint, we have $\hat{\Phi}_k = (\mathbf{A} + \lambda_{1k}\Omega)^{-1}a$ and $\hat{\Phi}_k^{-t_0} = (\mathbf{A} + \lambda_{1k}\Omega)^{-1}\tilde{a}(t_0)$. Consequently:

$$\hat{\phi}_{t_0k} - \hat{\phi}_{t_0k}^{-t_0} = [(\mathbf{A} + \lambda_{1k}\Omega)^{-1}]_{t_0t_0}(a_{t_0} - \tilde{a}_{t_0}(t_0)) = [(\mathbf{A} + \lambda_{1k}\Omega)^{-1}]_{t_0t_0}(a_{t_0} - \mathbf{A}_{t_0t_0}\hat{\phi}_{t_0k}^{-t_0}).$$

4. Finally, we obtain

$$\begin{aligned} \hat{\phi}_{t_0k} - \frac{a_{t_0}}{\mathbf{A}_{t_0t_0}} &= \hat{\phi}_{t_0k}^{-t_0} - \frac{a_{t_0}}{\mathbf{A}_{t_0t_0}} + [(\mathbf{A} + \lambda_{1k}\Omega)^{-1}]_{t_0t_0}(a_{t_0} - \mathbf{A}_{t_0t_0}\hat{\phi}_{t_0k}^{-t_0}) \\ \Rightarrow \hat{\phi}_{t_0k} - \frac{a_{t_0}}{\mathbf{A}_{t_0t_0}} &= (1 - \frac{\mathbf{A}_{t_0t_0}}{[(\mathbf{A} + \lambda_{1k}\Omega)^{-1}]_{t_0t_0}})(\hat{\phi}_{t_0k}^{-t_0} - \frac{a_{t_0}}{\mathbf{A}_{t_0t_0}}) \end{aligned}$$

$$\text{Hence, we have } \frac{\mathbf{A}_{t_0,t_0} \left(\hat{\phi}_{t_0k} - \frac{a_{t_0}}{\mathbf{A}_{t_0,t_0}} \right)^2}{\left(1 - [(\mathbf{A} + \lambda_{1k}\Omega)^{-1}]_{t_0t_0} \right)^2} = \mathbf{A}_{t_0,t_0} \left(\hat{\phi}_{t_0k}^{-t_0} - \frac{a_{t_0}}{\mathbf{A}_{t_0,t_0}} \right)^2.$$

A.4 Generation of randomized covariates for testing

In the simulations and real data examples, we encounter two types of Z_j : Gaussian and binary. We model the conditional distribution of Z_j given Z_{j^c} with a (penalized) GLM. For Gaussian data, we consider a model where

$$Z_j = Z_{j^c}\theta + \epsilon_j, \quad \epsilon_j \sim \mathcal{N}(0, \sigma^2).$$

We estimate θ and σ^2 empirically from data. When q , the dimension of Z , is large, we apply a lasso penalty on β with penalty level selected with cross-validation. Let $\hat{\theta}$ and $\hat{\sigma}^2$ be our estimates of the distribution parameters. We then generate new \mathbf{z}_i^* for subject

i from the estimated distribution $\mathbf{z}_i^* = \mathbf{z}_{i,j^c}^\top \hat{\theta} + \epsilon_{ij}^*$, with ϵ_{ij}^* independently generated from $\mathcal{N}(0, \hat{\sigma}^2)$. For binary Z_j , we consider the model

$$\log \frac{P(Z_j = 1)}{1 - P(Z_j = 1)} = Z_{j^c} \theta.$$

Again, we estimate θ empirically, with cross-validated lasso penalty for large q . We then generate z_{ij}^* independently from

$$P(Z_j = 1 | \mathbf{z}_{j^c}) = \frac{1}{1 + \exp(-\mathbf{z}_{i,j^c}^\top \hat{\theta})}.$$

To generate Z_j^* from the marginal distribution of Z_j , instead of estimating this distribution, we let \mathbf{Z}_j^* be a random permutation of \mathbf{Z}_j .

The randomization test requires generating Z_j^* from the conditional or marginal distribution of Z_j , and estimating the resulting distribution of T^* . We will estimate the distribution of T^* by fitting a skewed t-distribution as suggested in (Katsevich and Roeder, 2020). The use of the fitted $\hat{G}(\cdot)$ instead of the naive empirical CDF can greatly reduce the computational cost: We may obtain accurate estimates of small p-values around 10^{-4} using only 200 independent generations of Z_j^* and the fitted $\hat{G}(\cdot)$.

B Proofs

B.1 Proof of Theorem 3.1

The first step leads to non-decreasing marginal log-likelihood by definition, while the second step is a EM procedure. If we can show that the penalized marginal log-likelihood is non-decreasing at each subroutine of the EM procedure, we prove Theorem 3.1.

For simplicity, θ be the parameters that is being updated in some subroutine and $\Theta_{\setminus \theta}$ parameters excluding θ . Let $\Theta = \Theta_{\setminus \theta} \cup \theta$, $\Theta' = \Theta_{\setminus \theta} \cup \theta'$. It is known that if a new θ' is no worse compared with θ using the EM objective, it is no worse than θ when it comes to the (regularized) marginal MLE (Dempster et al., 1977). We include the short proof here for completeness.

Because the log of the posterior of \mathbf{U} can be decomposed into the difference between the log of the log complete likelihood and the log marginal likelihood, $L(\mathbf{U} | \mathbf{X}, \Theta) = L(\mathbf{U}, \mathbf{X} | \Theta) - L(\mathbf{X} | \Theta)$, we have (expectation with respect to posterior distribution of \mathbf{U}

with parameters Θ):

$$\mathbb{E}_\Theta L(\mathbf{U}, \mathbf{X}|\Theta') = \mathbb{E}_\Theta L(\mathbf{X}|\Theta') + \mathbb{E}_\Theta L(\mathbf{U}|\mathbf{X}, \Theta') = L(\mathbf{X}|\Theta') + \mathbb{E}_\Theta L(\mathbf{U}|\mathbf{X}, \Theta').$$

As a result, when

$$\mathbb{E}_\Theta L(\mathbf{X}, \mathbf{U}|\Theta') \geq \mathbb{E}_\Theta L(\mathbf{X}, \mathbf{U}|\Theta),$$

the following inequality holds,

$$\begin{aligned} L(\mathbf{X}|\Theta') - L(\mathbf{X}|\Theta) &= \{\mathbb{E}_\Theta L(\mathbf{X}|\Theta') + \mathbb{E}_\Theta L(\mathbf{U}|\mathbf{X}, \Theta') - L(\mathbf{X}|\Theta')\} + \{\mathbb{E}_\Theta L(\mathbf{U}|\mathbf{X}, \Theta') - \mathbb{E}_\Theta L(\mathbf{U}|\mathbf{X}, \Theta)\} \\ &\geq \mathbb{E}_\Theta \log \frac{P(\mathbf{U}|\mathbf{X}, \Theta)}{P(\mathbf{U}|\mathbf{X}, \Theta')} \geq 0. \end{aligned}$$

The last inequality is due to the fact that the mutual information $\mathbb{E}_\Theta \log \frac{P(\mathbf{U}|\mathbf{X}, \Theta)}{P(\mathbf{U}|\mathbf{X}, \Theta')}$ is non-negative. Now, we return to our subroutines for updating parameters $(\mathbf{V}, \Phi, s^2, \sigma^2)$:

- For our subroutines of updating s^2 and σ^2 , they are defined as the maximizers of $\mathbb{E}_\Theta L(\mathbf{X}, \mathbf{U}|\Theta_{-\theta}, \theta)$.
- From the proof to Lemma A.1 in deriving the explicit form for updating Φ and \mathbf{V} (see section), we know that $J(\mathbf{V}_k)$ is a convex quadratic loss and $J(\mathbf{V}_k) = \sum_{j=1}^J (a_{jk}v_{jk}^2 + b_{jk}v_{jk})$ for coefficients with explicit forms. If we can show that

$$\mathbf{V}_k \leftarrow \min_{\mathbf{V}_k} J(\mathbf{V}_k) + \nu \|\mathbf{V}_k\|_2^2 \quad \|\mathbf{V}_k\|_2^2 = 1,$$

is an minimizer to the problem $\{\min_{\mathbf{V}_k} J(\mathbf{V}_k), \text{ s.t. } \|\mathbf{V}_k\|_2^2 = 1\}$, then updating \mathbf{V}_k to this new vector is valid and will not increase our loss. This is true by standard optimization arguments. Let $L(\mathbf{V}_k, \nu) = \min_{\mathbf{V}_k} \max_{\nu} [J(\mathbf{V}_k) + \nu(\|\mathbf{V}_k\|_2^2 - 1)]$. Let ν be such a value such that $\|\mathbf{V}_k\|_2^2 = 1$, and let \mathbf{V}_k^* be the solution at this ν . Then,

$$J(\mathbf{V}_k^*) = \min_{\mathbf{V}_k} L(\mathbf{V}_k, \nu) \leq \min_{\mathbf{V}_k} \max_{\nu} L(\mathbf{V}_k, \nu) = \min_{\|\mathbf{V}_k\|_2^2} J(\mathbf{V}_k) \leq J(\mathbf{V}_k^*).$$

Hence, the proposed strategy at line 5 in Algorithm 1 solves the original problem.

The same arguments hold for updating Φ_k .

Hence, given Θ^ℓ the posterior distribution at the beginning of iteration ℓ , if we update the model parameters at proposed to acquire $\Theta^{\ell+1}$, we always have $J(\Theta^{\ell+1}) \leq J(\Theta^\ell)$.

B.2 Proof of Lemma 4.1

Statement I: Suppose $\mathbf{X}_I = \mathbf{U}_\perp \mathbf{M}_U^\top$, $\mathbf{X}_T = \Phi_\perp \mathbf{M}_T^\top$ and $\mathbf{X}_V = \mathbf{V}_\perp^\top \mathbf{M}_V$ for some matrices \mathbf{M}_U , \mathbf{M}_T , \mathbf{M}_V . Then, there exists a rank- K core-array $\mathbf{G} = \sum_{k=1}^K \mathbf{A}_k \odot \mathbf{B}_k \odot \mathbf{C}_k$, such that $\mathbf{U} = \mathbf{U}_\perp \mathbf{A}$, $\Phi = \Phi_\perp \mathbf{B}$ and $\mathbf{V} = \mathbf{V}_\perp \mathbf{C}$ form a PARAFAC decomposition of \mathbf{X} :

$$\mathbf{X} = \sum_{k=1}^K \mathbf{U}_k \odot \Phi_k \odot \mathbf{V}_k.$$

Argument I: Statement I can be checked easily: since \mathbf{U}_\perp spans the row space of \mathbf{X}_I , we can find a matrix \mathbf{A} such that if we replace \mathbf{U}^* with $\mathbf{U}_\perp \mathbf{A}$, we still have a PARAFAC decomposition of \mathbf{X} . We can apply the same arguments to Φ_\perp , \mathbf{V}_\perp , and hence prove the statement at the beginning.

As a result, we need to show that \mathbf{U}_\perp , Φ_\perp and \mathbf{V}_\perp spans the column spaces of the three unfolding matrices and $\tilde{\mathbf{G}}$ is the unfolding of such a core array along the subject dimension.

- The proposed \mathbf{V}_\perp satisfies the requirement by construction. Hence, we need only to check that \mathbf{U}_\perp and Φ_\perp spans the row space of \mathbf{X}_I and \mathbf{X}_T respectively.
- The projection of \mathbf{X}_J onto \mathbf{V}_\perp results in $\mathbf{H} = \mathbf{V}_\perp^\top \mathbf{X}_j = \mathbf{C}(\Phi^* \odot \mathbf{U}^*)^\top$, where $\mathbf{C} = \mathbf{V}_\perp^\top \mathbf{V}^*$. Hence, we have

$$\mathbf{W} = \sum_{k=1}^K \frac{1}{I} \mathbf{Y}(k)^\top \mathbf{Y}(k) = \Phi^* \left(\sum_{k=1}^K (\mathbf{U}^* \cdot \mathbf{C}_{k,\cdot})^\top (\mathbf{U}^* \cdot \mathbf{C}_{k,\cdot}) \right) \Phi^{*,T} = \Phi^* \mathbf{M} \Phi^{*\top}$$

where $\mathbf{M} = \mathbb{R}^{K \times K}$ with $M_{\ell k} = \langle \mathbf{C}_\ell, \mathbf{C}_k \rangle \langle \mathbf{U}_\ell^*, \mathbf{U}_k^* \rangle$. Notice that

$$\begin{aligned} \mathbf{X}_T \mathbf{X}_T^\top &= \Phi^* (\mathbf{V}^* \odot \mathbf{U}^*)^\top (\mathbf{V}^* \odot \mathbf{U}^*) \Phi^{*,T} \\ &= \Phi^* ((\mathbf{V}_\perp \mathbf{C}_1) \otimes \mathbf{U}_1^*, \dots, (\mathbf{V}_\perp \mathbf{C}_K) \otimes \mathbf{U}_K^*)^\top ((\mathbf{V}_\perp \mathbf{C}_1) \otimes \mathbf{U}_1^*, \dots, (\mathbf{V}_\perp \mathbf{C}_K) \otimes \mathbf{U}_K^*) \Phi^{*\top} \\ &= \Phi^* ((\mathbf{C}_\ell^\top \mathbf{V}_\perp^\top \mathbf{V}_\perp \mathbf{C}_k) \otimes (\mathbf{U}_\ell^\top \mathbf{U}_k))_{\ell k} \Phi^{*\top} \\ &= \Phi^* ((\mathbf{C}_\ell^\top \mathbf{C}_k) (\mathbf{U}_\ell^\top \mathbf{U}_k))_{\ell k} \Phi^{*\top} = \Phi^* \mathbf{M} \Phi^{*\top} \end{aligned}$$

Hence, Φ_\perp is the top K left singular vectors of \mathbf{X}_T . We set $\mathbf{B} = \Phi_\perp^\top \Phi^*$.

- $\tilde{\mathbf{U}}$ is estimated by regression \mathbf{X}_I on $\mathbf{V}_\perp \otimes \Phi$. Because both \mathbf{V}_\perp and Φ_\perp are orthonormal, $\mathbf{V}_\perp \otimes \Phi_\perp$ is also orthonormal:

$$(\mathbf{V}_\perp \otimes \Phi)^\top (\mathbf{V}_\perp \otimes \Phi) = (\mathbf{V}_\perp^\top \mathbf{V}_\perp) \otimes (\Phi^\top \Phi_\perp) = \mathbf{Id}_{K \times K} \otimes \mathbf{Id}_{K \times K} = \mathbf{Id}_{K^2 \times K^2}.$$

Hence, we have

$$\begin{aligned}
\tilde{\mathbf{U}}(\mathbf{V}_\perp \otimes \mathbf{\Phi}_\perp)^\top &= \frac{1}{1+\delta} \mathbf{X}_I(\mathbf{V}_\perp \otimes \mathbf{\Phi}_\perp)(\mathbf{V}_\perp \otimes \mathbf{\Phi}_\perp)^\top \\
&= \frac{1}{1+\delta} \mathbf{X}_I((\mathbf{V}_\perp \mathbf{V}_\perp^\top) \otimes (\mathbf{\Phi}_\perp \mathbf{\Phi}_\perp^\top)) \\
&= \frac{1}{1+\delta} \mathbf{U}^* ((\mathbf{V}_\perp \mathbf{C}) \odot (\mathbf{\Phi}_\perp \mathbf{B}))^\top (\mathbf{V}_\perp \otimes \mathbf{\Phi}_\perp)(\mathbf{V}_\perp \otimes \mathbf{\Phi}_\perp)^\top \\
&= \mathbf{U}^* \begin{pmatrix} (\mathbf{C}_1^\top \mathbf{V}_\perp^\top \mathbf{V}_\perp \mathbf{V}_\perp^\top) \otimes (\mathbf{B}_1^\top \mathbf{\Phi}_\perp^\top \mathbf{\Phi}_\perp \mathbf{\Phi}_\perp^\top) \\ \dots \\ (\mathbf{C}_K^\top \mathbf{V}_\perp^\top \mathbf{V}_\perp \mathbf{V}_\perp^\top) \otimes (\mathbf{B}_K^\top \mathbf{\Phi}_\perp^\top \mathbf{\Phi}_\perp \mathbf{\Phi}_\perp^\top) \end{pmatrix} (\mathbf{V}_\perp \otimes \mathbf{\Phi}_\perp) \\
&= \frac{1}{1+\delta} \mathbf{X}_I
\end{aligned}$$

The row space spanned by $\tilde{\mathbf{U}}$ is the same as the row space spanned by \mathbf{X}_I , thus, the space spanned by top K left singular vectors of $\tilde{\mathbf{U}}$ is the same by that of \mathbf{X}_I . As a result, \mathbf{U}_\perp also satisfies the requirement.

- In particular, we also have

$$\mathbf{U}_\perp^\top \tilde{\mathbf{U}} = \frac{1}{1+\delta} \mathbf{U}_\perp^\top \mathbf{X}_I(\mathbf{V}_\perp \otimes \mathbf{\Phi}_\perp) = \frac{1}{1+\delta} \mathbf{U}_\perp^\top \mathbf{U}_\perp \mathbf{G}_I(\mathbf{V}_\perp \otimes \mathbf{\Phi}_\perp)^\top (\mathbf{V}_\perp \otimes \mathbf{\Phi}_\perp) = \mathbf{G}_I$$

where \mathbf{G}_I is the unfolding of the core array \mathbf{G} in the subject dimension. Hence, we recover $\mathbf{A}, \mathbf{B}, \mathbf{C}$ applying a rank-K PARAFAC decomposition on the arranged three-dimensional core array from \mathbf{G}_I as described in Algorithm 2.

B.3 Proof of Lemma 4.2

Let $\mathbf{e}_k = (\underbrace{0, \dots, 0}_{k-1}, 1, \underbrace{0, \dots, 0}_{K-k})^\top$. Plug-in the expression of $\mathbf{X}_{I,\vec{i}} = (\mathbf{V} \odot \Phi)_{\vec{i}} \mathbf{u}_i = (\mathbf{V} \odot \Phi)_{\vec{i}} ((\boldsymbol{\beta}^*)^\top \mathbf{z}_i + \zeta_i) + \epsilon_{I,\vec{i}}$ into the expression of $\tilde{y}_i(\delta)$:

$$\begin{aligned} \tilde{y}_i(\delta) &= \left((\boldsymbol{\Sigma}_i(\delta))_{k:} (\mathbf{V} \odot \Phi)^\top \Lambda_{\vec{i}} \mathbf{X}_{I,\vec{i}} + \delta \sum_{\ell \neq k} \frac{(\boldsymbol{\Sigma}_i(\delta))_{kl}}{s_\ell^2} \mathbf{z}_i^\top \boldsymbol{\beta}_\ell \right) \\ &= (\mathbf{e}_k^\top - \delta (\boldsymbol{\Sigma}_i(\delta))_{k:} \Lambda_f) (\boldsymbol{\beta}^*)^\top \mathbf{z}_i + \delta \sum_{\ell \neq k} \frac{(\boldsymbol{\Sigma}_i(\delta))_{kl}}{s_\ell^2} \mathbf{z}_i^\top \boldsymbol{\beta}_\ell + (\mathbf{e}_k^\top - \delta (\boldsymbol{\Sigma}_i(\delta))_{k:} \Lambda_f) \zeta_i \\ &\quad + (\boldsymbol{\Sigma}_i(\delta))_{k:} (\mathbf{V} \odot \Phi)_{\vec{i}}^\top \Lambda_{\vec{i}} \epsilon_{I,\vec{i}} \\ &= (1 - \delta \frac{(\boldsymbol{\Sigma}_i(\delta))_{kk}}{s_k^2}) \mathbf{z}_i^\top \boldsymbol{\beta}_k^* + \underbrace{\sum_{\ell \neq k} \frac{(\boldsymbol{\Sigma}_i(\delta))_{kl}}{s_\ell^2} \mathbf{z}_i^\top (\boldsymbol{\beta}_\ell - \boldsymbol{\beta}_\ell^*)}_{\Delta_i(\delta)} + \xi_i \end{aligned}$$

where $\xi_i = (\mathbf{e}_k^\top - \delta (\boldsymbol{\Sigma}_i(\delta))_{k:} \Lambda_f) \zeta_i + (\boldsymbol{\Sigma}_i(\delta))_{k:} (\mathbf{V} \odot \Phi)_{\vec{i}}^\top \Lambda_{\vec{i}} \epsilon_{I,\vec{i}}$ and

$$\begin{aligned} \mathbb{E}(\xi_i^2) &= (\mathbf{e}_k^\top - \delta (\boldsymbol{\Sigma}_i(\delta))_{k:} \Lambda_f) \Lambda_f^{-1} (\mathbf{e}_k - \delta \Lambda_f (\boldsymbol{\Sigma}_i(\delta))_{:k}) + (\boldsymbol{\Sigma}_i(\delta))_{k:} (\mathbf{V} \odot \Phi)_{\vec{i}}^\top \Lambda_{\vec{i}} (\mathbf{V} \odot \Phi)_{\vec{i}}^\top (\boldsymbol{\Sigma}_i(\delta))_{:k} \\ &= s_k^2 - 2\delta (\boldsymbol{\Sigma}_i(\delta))_{kk} + \delta^2 (\boldsymbol{\Sigma}_i(\delta))_{k:} \Lambda_f (\boldsymbol{\Sigma}_i(\delta))_{:k} (\delta) + (\boldsymbol{\Sigma}_i(\delta))_{k:} (\boldsymbol{\Sigma}_i^{-1} - \delta \Lambda_f) (\boldsymbol{\Sigma}_i(\delta))_{:k} \\ &= s_k^2 + (1 - 2\delta) (\boldsymbol{\Sigma}_i(\delta))_{kk} (\delta) + (\delta^2 - \delta) (\boldsymbol{\Sigma}_i(\delta))_{k:} \Lambda_f (\boldsymbol{\Sigma}_i(\delta))_{:k} = w_i(\delta) \end{aligned}$$

B.4 Proof of Lemma A.1

B.4.1 Update of $\boldsymbol{\beta}_k$:

From eq. (4) and eq. (5), update of $\boldsymbol{\beta}$ considers the objective:

$$\begin{aligned} J(\boldsymbol{\beta}) &= \frac{1}{2} \mathbf{f}_i^\top \left(\Lambda_{\vec{i}}^{-1} - \Lambda_{\vec{i}}^{-1} \mathbf{H}_{\vec{i}} \boldsymbol{\Sigma}_i \mathbf{H}_{\vec{i}}^\top \Lambda_{\vec{i}}^{-1} \right) \mathbf{f}_i + \sum_k \lambda_{2k} |\boldsymbol{\beta}_k| \\ &= \frac{1}{2} \left[\boldsymbol{\eta}_i^\top M^i \boldsymbol{\eta}_i + \mathbf{X}_{I\vec{i}}^\top \left(\Lambda_{\vec{i}}^{-1} - \Lambda_{\vec{i}}^{-1} \mathbf{H}_{\vec{i}} \boldsymbol{\Sigma}_i \mathbf{H}_{\vec{i}}^\top \Lambda_{\vec{i}}^{-1} \right) \mathbf{X}_{I\vec{i}} + 2 \boldsymbol{\eta}_i^\top m^i \right] + \sum_k \lambda_{2k} |\boldsymbol{\beta}_k|, \end{aligned} \tag{17}$$

where

$$\begin{aligned} \boldsymbol{\eta}_i &= \boldsymbol{\beta}^\top \mathbf{z}_i, \\ M^i &= \Lambda_f^{-1} - \Lambda_f^{-1} \boldsymbol{\Sigma}_i \Lambda_f^{-1}, \\ m^i &= \Lambda_f^{-1} \boldsymbol{\Sigma}_i \mathbf{H}_{\vec{i}}^\top \Lambda_{\vec{i}}^{-1} \mathbf{X}_{I\vec{i}}. \end{aligned}$$

Hence, for β_k , we consider the following minimization problem

$$\begin{aligned} J(\beta_k) &= \frac{1}{2} \left[\beta_k^\top z_i^\top M_{kk}^i z_i \beta_k - 2\beta_k^\top z_i^\top \left(m_k^i - \sum_{\ell \neq k} M_{k\ell}^i z_i \beta_\ell \right) \right] + \lambda_{2k} |\beta_k|, \\ &= \beta_k^\top \underbrace{\tilde{z}_i^\top \tilde{z}_i \beta_k - 2\beta_k^\top \tilde{z}_i^\top (M_{kk}^i)^{-\frac{1}{2}} \left(m_k^i - \sum_{\ell \neq k} M_{k\ell}^i z_i \beta_\ell \right)}_{\tilde{y}_i}. \end{aligned}$$

It is straightforward to check that the definitions of \tilde{z}_i and \tilde{y}_i are the same as the ones used in Lemma A.1.

B.4.2 Update of \mathbf{V}_k and Φ_k :

We can rewrite the complete log-likelihood using the unfolding along the feature dimension and the time dimension. The relevant terms to \mathbf{V} and Φ are:

$$\begin{aligned} L(\mathbf{X}, \mathbf{U} | \Theta) &= -\frac{1}{2} \sum_j \left(\mathbf{X}_{J,\vec{j}} - (\Phi \odot \mathbf{U})_{\vec{j}} \mathbf{v}_j \right)^\top \Lambda_{\vec{j}}^{-1} \left(\mathbf{X}_{J,\vec{j}} - (\Phi \odot \mathbf{U})_{\vec{j}} \mathbf{v}_j \right), \\ &= -\frac{1}{2} \sum_t \left(\mathbf{X}_{T,\vec{t}} - (\mathbf{V} \odot \mathbf{U})_{\vec{t}} \phi_j \right)^\top \Lambda_{\vec{t}}^{-1} \left(\mathbf{X}_{J,\vec{j}} - (\mathbf{V} \odot \mathbf{U})_{\vec{t}} \phi_j \right). \end{aligned}$$

Let $O_{it} = 1$ if observation time index t for subject i is available, and let o_i be the set of index where $O_{it} = 1$ for subject i . By direct calculation, the expectation of the negative log-likelihood (keeping only terms relevant to Φ and \mathbf{V}) are given below:

$$\begin{aligned} &\frac{1}{2} \mathbb{E} \left[\sum_j \left(\mathbf{X}_{J,\vec{j}} - (\Phi \odot \mathbf{U})_{\vec{j}} \mathbf{v}_j \right)^\top \Lambda_{\vec{j}}^{-1} \left(\mathbf{X}_{J,\vec{j}} - (\Phi \odot \mathbf{U})_{\vec{j}} \mathbf{v}_j \right) \right], \\ &\propto \frac{1}{2} \sum_j \sum_i \left(-2\mathbf{X}_{ij,o_i}^\top \Lambda_{\vec{j}}^{-1} (\Phi_{o_i} \odot \langle \mathbf{u}_i \rangle) \mathbf{v}_j + \mathbf{v}_j^\top \left(\Phi_{o_i}^\top \Lambda_{\vec{j}}^{-1} \Phi_{o_i} \cdot \langle \mathbf{u}_i \mathbf{u}_i^\top \rangle \right) \mathbf{v}_j \right). \end{aligned} \quad (18)$$

$$\begin{aligned} &\frac{1}{2} \mathbb{E} \left[\sum_t \left(\mathbf{X}_{T,\vec{t}} - (\mathbf{V} \odot \mathbf{U})_{\vec{t}} \phi_t \right)^\top \Lambda_{\vec{t}}^{-1} \left(\mathbf{X}_{T,\vec{t}} - (\mathbf{V} \odot \mathbf{U})_{\vec{t}} \phi_t \right) \right], \\ &\propto \frac{1}{2} \sum_t \sum_{i: O_{it}=1} \left(-2\mathbf{X}_{i,.,t}^\top \Lambda_{\vec{t}}^{-1} (\mathbf{V} \odot \langle \mathbf{u}_i \rangle) \phi_t + \phi_t^\top \left(\mathbf{V}^\top \Lambda_{\vec{t}}^{-1} \mathbf{V} \cdot \langle \mathbf{u}_i \mathbf{u}_i^\top \rangle \right) \phi_t \right). \end{aligned} \quad (19)$$

Update \mathbf{V}_k : From eq. (18), update of \mathbf{V}_k considers the following problem

$$\min_{\mathbf{V}_k} J(\mathbf{V}_k) = \sum_{j=1}^J \frac{1}{2} (a_{jk} v_{jk}^2 - 2b_{jk} v_{jk}), \quad s.t. \quad \|\mathbf{V}_k\|_2^2 = 1.$$

Here, a_{jk} and b_{jk} are defined below:

$$\begin{aligned} a_{jk} &= \frac{1}{\sigma_j^2} \sum_{i,t:O_{it}=1} (\phi_{tk}^2 \langle u_{ik} \rangle^2 + \Sigma_{kk}^i \phi_{tk}^2), \\ &= \sum_{i,t:O_{it}=1} (\phi_{tk}^2 \langle u_{ik}^2 \rangle) = \langle \|(\mathbf{U} \odot \Phi)_{\vec{j},k}\|_2^2 \rangle. \\ b_{jk} &= \frac{1}{\sigma_j^2} \sum_{i,t:O_{itj}=1} \left(\left(x_{ijt} - \sum_{k' \neq k} v_{jk'} \phi_{tk'} \langle \mathbf{u}_{ik'} \rangle \right) \langle \mathbf{u}_{ik} \rangle \phi_{tk} - \sum_{k' \neq k} \Sigma_{kk'}^i v_{jk'} \phi_{tk'} \phi_{tk} \right). \end{aligned}$$

Hence, if we set Q_1 , Q_2 , Q_3 as specified, we have $a_{jk} = \frac{1}{\sigma_j^2} \|Q_{1,\vec{j},k}\|_2^2 + Q_{3kk,j}$ and $b_{jk} = Q_{2kj} - \sum_{k' \neq k} Q_{3kk'} v_{jk'}$.

Update Φ_k Updating Φ_k is similar to updating \mathbf{V}_k apart from the inclusion of the smoothness regularizer. Set $Q_1 = \langle \mathbf{U} \rangle \odot \Phi \in \mathbb{R}^{IT \times K}$, $Q_2 \in \mathbb{R}^{K \times T}$ and $Q_3 \in \mathbb{R}^{K \times K \times T}$ with

$$\begin{aligned} Q_{2kt} &= \mathbf{X}_{Tt}^\top \text{diag}\left\{\frac{1}{\sigma_t^2}\right\} Q_{1\vec{t}k} \\ Q_{3k_1 k_2 t} &= \sum_j \frac{1}{\sigma_j^2} v_{jk_1} v_{jk_2} \sum_{i:O_{it}=1} (\Sigma_{ik_1 k_2} + \langle u_{ik_1} \rangle \langle u_{ik_2} \rangle) \end{aligned}$$

Then,

$$J(\Phi_k) = \sum_{t=1}^T \frac{1}{2} (a_{jk} v_{jk}^2 - 2b_{jk} v_{jk}) + \lambda_{1k} \Phi_k^\top \Omega \Phi_k,$$

where $a_{tk} = \left(\|\text{diag}\{\frac{1}{\sigma_t^2}\} Q_{1,\vec{t},k}\|_2^2 + Q_{3kk,t} \right)$ and $b_{jk} = \left(Q_{2kt} - \sum_{k' \neq k} Q_{3kk'} \phi_{tk'} \right)$.

B.4.3 Update of σ_j^2 and s_k^2

Since the expected log likelihood related to $\{s_k^2, k = 1, \dots, K\}$ is

$$\begin{aligned} &\frac{1}{2} \sum_{i=1}^I \{ \mathbb{E}_{\Theta_0} [-(\mathbf{u}_i - \boldsymbol{\beta}^\top \mathbf{z}_i)^\top \Lambda_f^{-1} (\mathbf{u}_i - \boldsymbol{\beta}^\top \mathbf{z}_i)] - \log |\Lambda_f| \} \\ &= \sum_{k=1}^K - \left\{ \frac{\sum_{i=1}^I ((\mu_{ik} - \mathbf{z}_i^\top \boldsymbol{\beta}_k)^2 + (\boldsymbol{\Sigma}_i)_{kk})}{s_k^2} + I \log s_k^2 \right\} \end{aligned}$$

Consequently, the solution for s_k^2 given other parameters is $s_k^2 = \frac{1}{I} \sum_{i=1}^I ((\mu_{ik} - \mathbf{z}_i^\top \boldsymbol{\beta}_k)^2 + (\boldsymbol{\Sigma}_i)_{kk})$.

the expected log likelihood related to $\{\sigma_j^2, j = 1, \dots, p\}$ is

$$-\frac{1}{2} \sum_{j=1}^J \left\{ \frac{1}{\sigma_j^2} \left[(X_{J,\vec{j}} - (\Phi \odot \mu)_{\vec{j}} \mathbf{v}_j)^\top (X_{J,\vec{j}} - (\Phi \odot \mu)_{\vec{j}} \mathbf{v}_j) + \mathbf{v}_j^\top \left(\sum_t \left(\sum_{O_{it}=1} \boldsymbol{\Sigma}_i \right) \cdot (\phi_t \phi_t^\top) \right) \mathbf{v}_j \right] + |\vec{j}| \log \sigma_j^2 \right\}$$

Consequently, the updating rule σ_h^2 given other parameters is

$$\sigma_j^2 = \frac{1}{|\vec{j}|} \left[(X_{J,\vec{j}} - (\Phi \odot \mu)_{\vec{j}} \mathbf{v}_j)^\top (X_{J,\vec{j}} - (\Phi \odot \mu)_{\vec{j}} \mathbf{v}_j) + \mathbf{v}_j^\top \left(\sum_t \left(\sum_{O_{it}=1} \Sigma_i \right) \cdot (\phi_t \phi_t^\top) \right) \mathbf{v}_j \right].$$

C Additional numerical results

C.1 Comparison of two initialization strategies

Fig.7 compares the achieved correlations with the signal tensor when SupCP are initialized using the proposed initialization method (referred to as SupCP) and the random initialization method (referred to as SupCP_random) (Lock and Li, 2018). The proposed strategy shows a clear gain in the setting of high missing rate or weak signal.

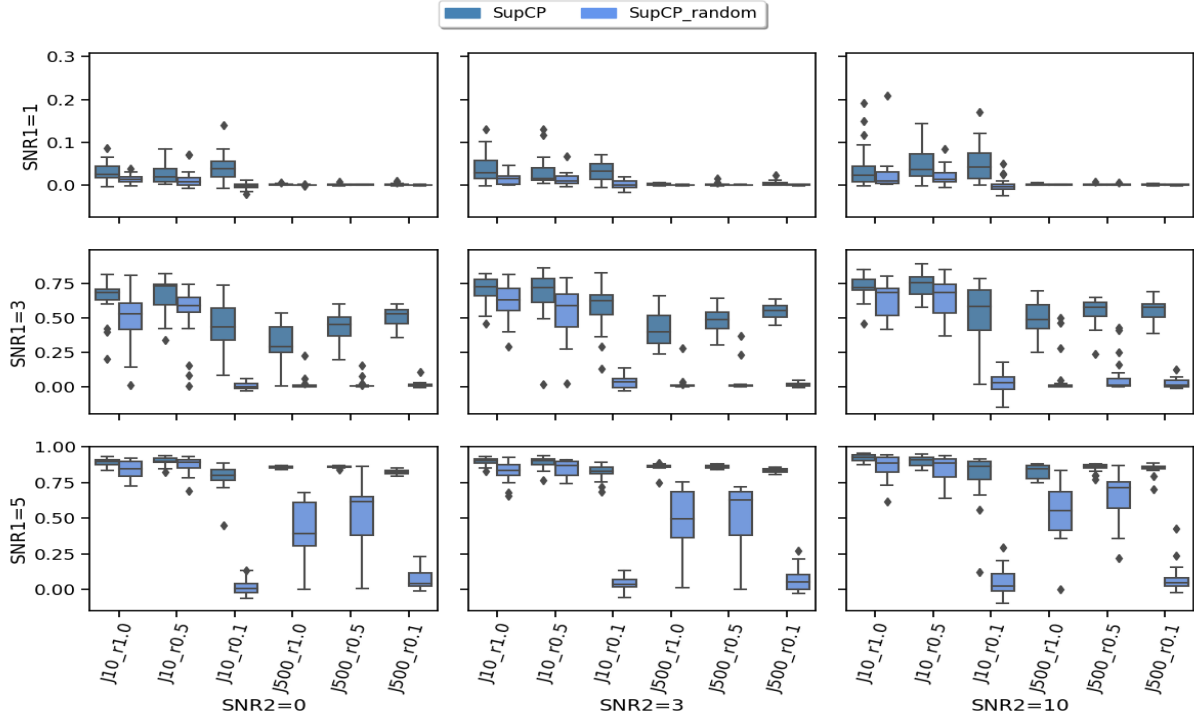


Figure 7: Reconstruction evaluation of the underlying signal tensor using different initializations in SupCP, measured by the correlations. In each subplot, x axis label indicates different J and observing rate, the y axis is the achieved correlation, and the box colors represent different methods. The corresponding subplot column/row name represents the signal-to-noise ratio SNR1/SNR2.

C.2 Signal reconstruction on missing entries

Fig.8 compares the achieved correlations with the signal tensor using different methods, but only on those missing entries. The proposed strategy shows a clear gain in the setting of high missing rate or weak signal. Consistent with Fig.1, SPACO improves over SPACO- with high SNR2, and is much better than SupCP or CP when the signal size SNR1 is weak (but still estimable using SPACO) or when the missing rate is high.

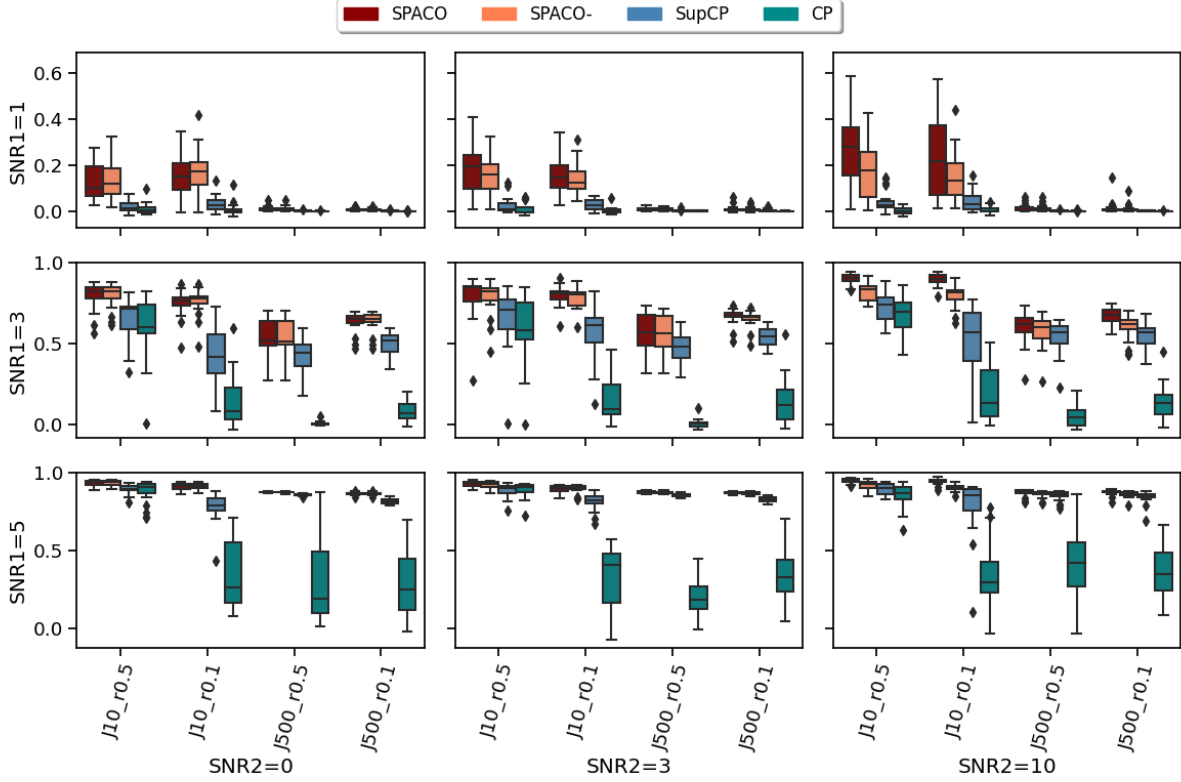


Figure 8: Reconstruction evaluation on missing entries by the correlations between the estimates and the true signal tensor. In each subplot, x axis label indicates different J and observing rate, the y axis is the achieved correlation, and the box colors represent different methods. The corresponding subplot column/row name represents the signal-to-noise ratio SNR1/SNR2.

C.3 Type I error with observing rate $r = 1.0, 0.1$

Figure 9: Achieved type I errors at observing rate $r = 1.0$. In each subplot, x axis label indicates different combination of feature dimension J and targeted level $\alpha \in \{0.01, 0.05\}$, the y axis is the achieved type I errors. Different bar colors represent different tests (partial or marginal). The two dashed horizontal lines indicate levels 0.01 and 0.05.

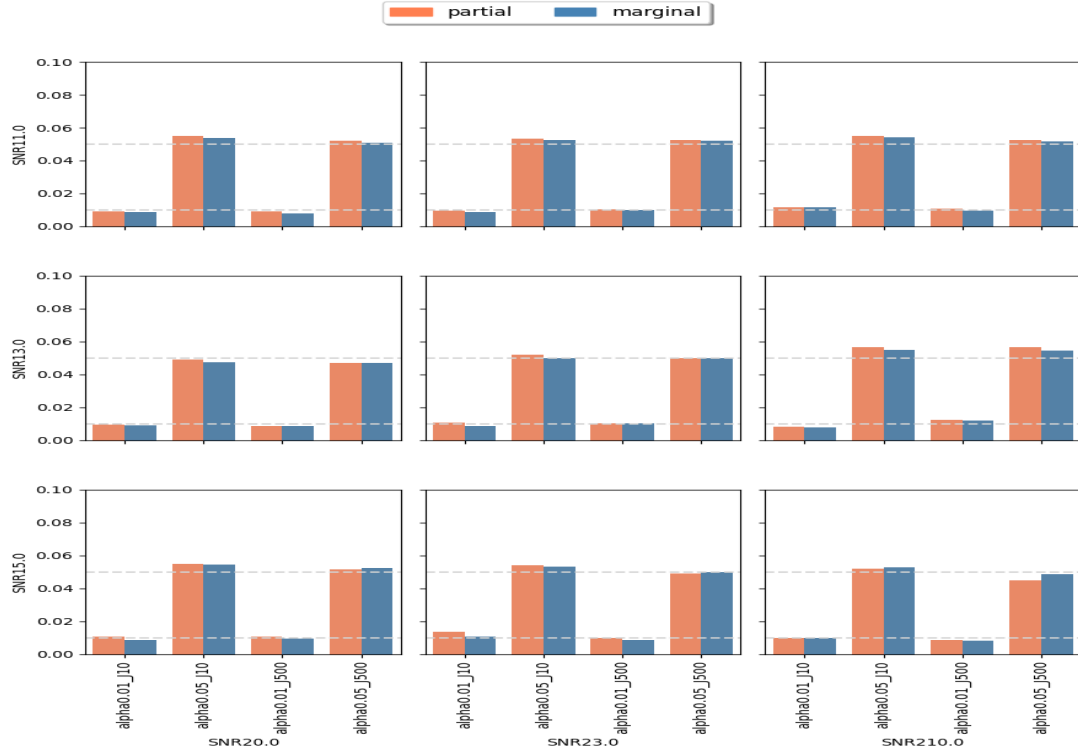
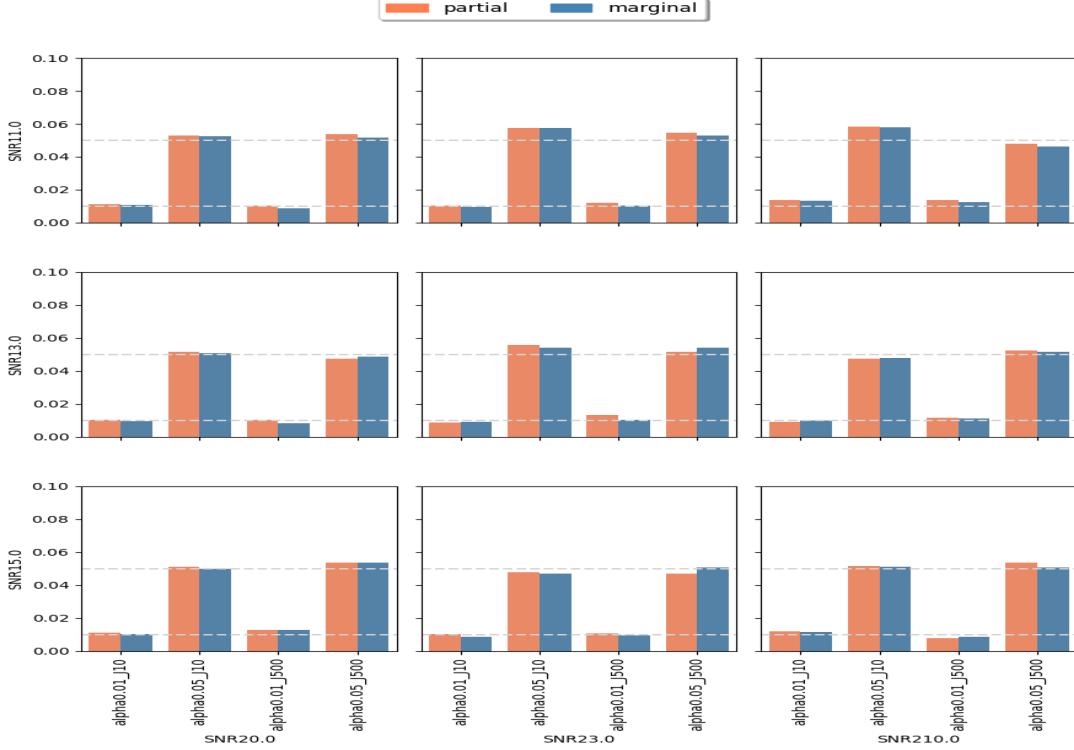


Figure 10: Achieved type I errors at observing rate $r = 0.1$. In each subplot, x axis label indicates different combination of feature dimension J and targeted level $\alpha \in \{0.01, 0.05\}$, the y axis is the achieved type I errors. Different bar colors represent different tests (partial or marginal). The two dashed horizontal lines indicate levels 0.01 and 0.05.



C.4 empirical p-value: cross-fit vs naive fit

In this section, we show qq-plots of the negative $\log_{10}(\text{pvalue})$ from the null hypotheses against its theoretical values from the uniform distribution. In Fig.11-Fig.13, we show the results from observing rate $r = 1.0, 0.5, 0.1$ respectively, and the red/blue points represent those from the cross fit and the full fit with blue diagonal representing the expected theoretical behavior. The sub-title indicates the dimensionality J , observing rate $r \in \{1.0, 0.5, 0.1\}$ and the type of estimate: `partial_fitted` means p values from partial independence test with p-value estimated using nct distribution and `marginal_fitted` means p values from marginal independence test with p-value estimated using nct distribution. The number of random-

ization used here is $B = 200$. We observe that direct plug-in of model parameters from full fit leads to poor performance when the signal-to-noise ratio is low. When $\text{SNR1} = 1$, the log pvalue is severely inflated based on the full fit, the cross-fit provides much uniform null p-value distribution even with only a five-step update.

Figure 11: qq-plots of constructed p-values at $r = 1.0$. The p values are estimated with net distribution. The red/blue points represent those from the cross-fit and the naive procedure, with blue diagonal representing the expected theoretical behavior.

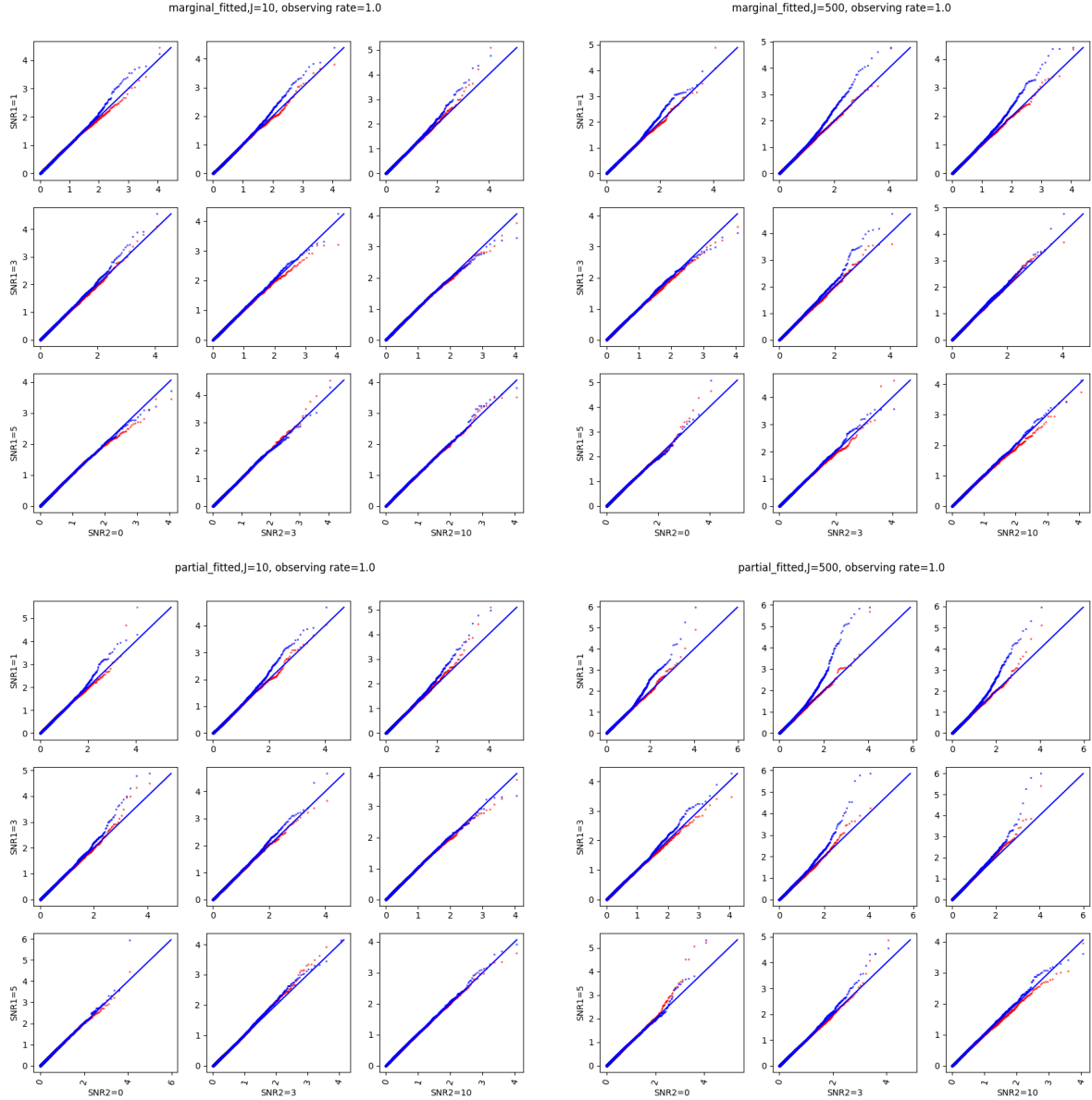


Figure 12: qq-plots of constructed p-values at $r = 0.5$. The p values are estimated with nct distribution. The red/blue points represent those from the cross-fit and the naive procedure, with blue diagonal representing the expected theoretical behavior.

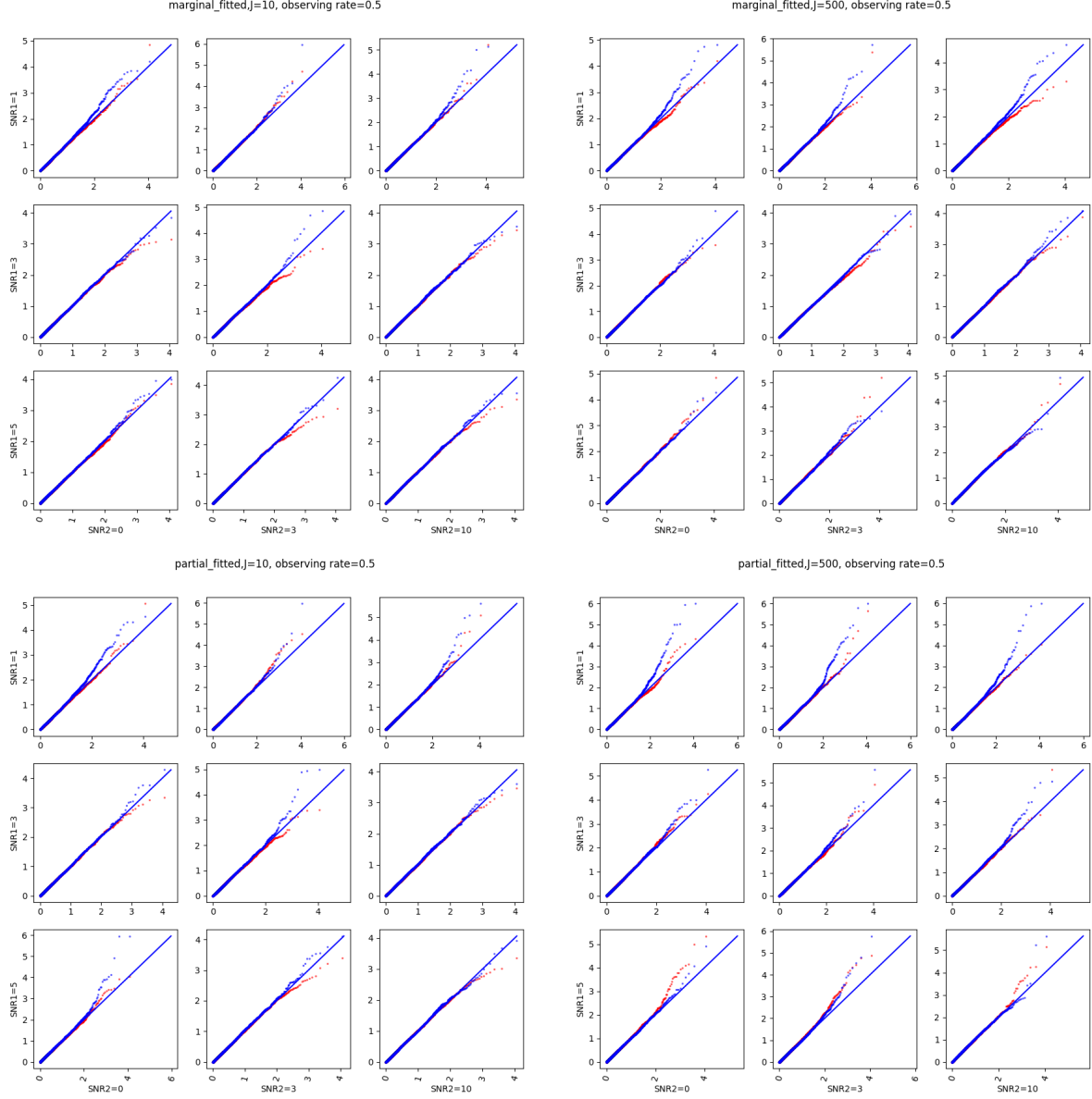
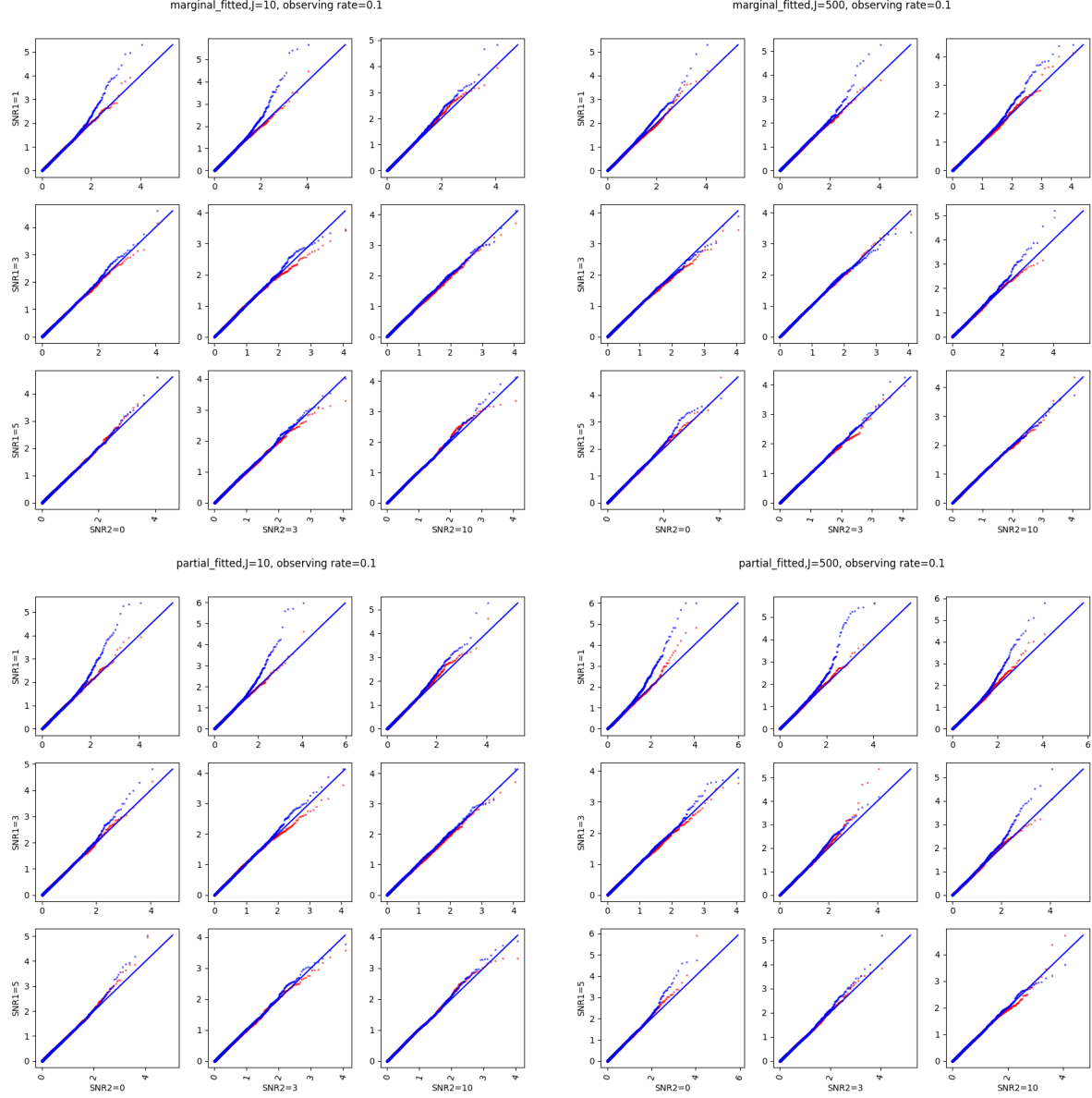
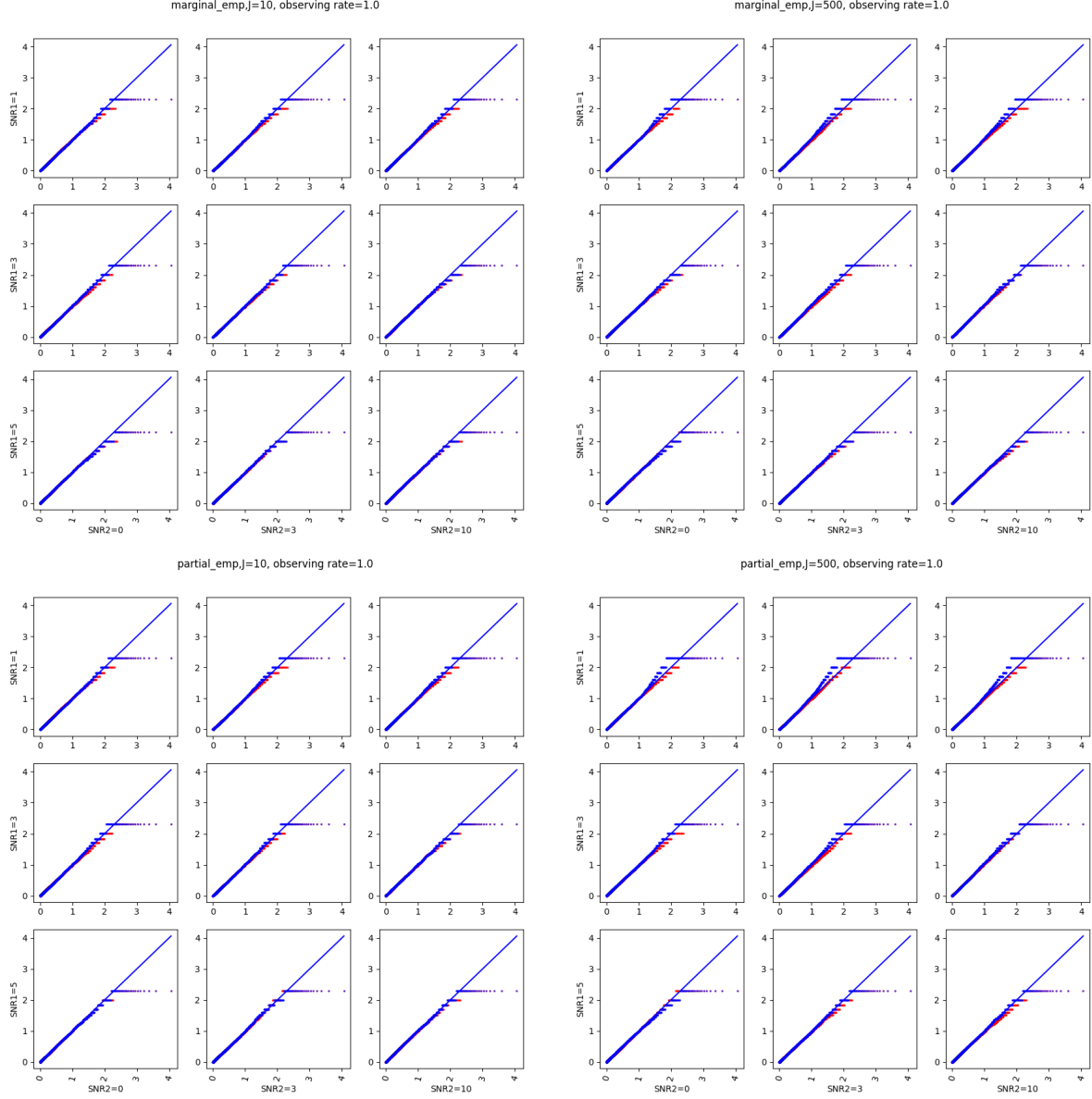


Figure 13: qq-plots of constructed p-values at $r = 0.1$. The p values are estimated with nct distribution. The red/blue points represent those from the cross-fit and the naive procedure, with blue diagonal representing the expected theoretical behavior.



When $B = 200$, the non-parametric estimate of the p values has a lower bound of $\frac{1}{B+1} = \frac{1}{201}$, but the nct-estimated p values do not have such a restriction. Fig.14 shows the non-parametric p value estimates at $r = 1.0$, we can easily show that the nct-estimated version provides more details for small p-values.

Figure 14: qq-plots of constructed p-values at $r = 1.0$. The p values are estimated directly from the empirical distribution. The red/blue points represent those from the cross-fit and the naive procedure, with blue diagonal representing the expected theoretical behavior.



References

- Acar, E. and B. Yener (2008). Unsupervised multiway data analysis: A literature survey. *IEEE transactions on knowledge and data engineering* 21(1), 6–20.

- Argelaguet, R., B. Velten, D. Arnol, S. Dietrich, T. Zenz, J. C. Marioni, F. Buettner, W. Huber, and O. Stegle (2018). Multi-omics factor analysis—a framework for unsupervised integration of multi-omics data sets. *Molecular systems biology* 14(6), e8124.
- Bai, J. and P. Wang (2016). Econometric analysis of large factor models. *Annual Review of Economics* 8, 53–80.
- Besse, P. and J. O. Ramsay (1986). Principal components analysis of sampled functions. *Psychometrika* 51(2), 285–311.
- Bro, R. and C. A. Andersson (1998). Improving the speed of multiway algorithms: Part ii: Compression. *Chemometrics and intelligent laboratory systems* 42(1-2), 105–113.
- Candès, E., Y. Fan, L. Janson, and J. Lv (2018). Panning for gold: ‘model-x’ knockoffs for high dimensional controlled variable selection series b statistical methodology.
- Carroll, J. D., S. Pruzansky, and J. B. Kruskal (1980). Candelinc: A general approach to multidimensional analysis of many-way arrays with linear constraints on parameters. *Psychometrika* 45(1), 3–24.
- De Lathauwer, L., B. De Moor, and J. Vandewalle (2000). A multilinear singular value decomposition. *SIAM journal on Matrix Analysis and Applications* 21(4), 1253–1278.
- Dempster, A. P., N. M. Laird, and D. B. Rubin (1977). Maximum likelihood from incomplete data via the em algorithm. *Journal of the Royal Statistical Society: Series B (Methodological)* 39(1), 1–22.
- Fan, J., Y. Fan, and J. Lv (2008). High dimensional covariance matrix estimation using a factor model. *Journal of Econometrics* 147(1), 186–197.
- Fan, J., Y. Liao, and M. Mincheva (2011). High dimensional covariance matrix estimation in approximate factor models. *Annals of statistics* 39(6), 3320.
- Harshman, R. A. and M. E. Lundy (1994). Parafac: Parallel factor analysis. *Computational Statistics & Data Analysis* 18(1), 39–72.

- Hinrich, J. L. and M. Mørup (2019). Probabilistic tensor train decomposition. In *2019 27th European Signal Processing Conference (EUSIPCO)*, pp. 1–5. IEEE.
- Huang, J. Z., H. Shen, A. Buja, et al. (2008). Functional principal components analysis via penalized rank one approximation. *Electronic Journal of Statistics* 2, 678–695.
- Imaizumi, M. and K. Hayashi (2017). Tensor decomposition with smoothness. In *International Conference on Machine Learning*, pp. 1597–1606. PMLR.
- Katsevich, E. and K. Roeder (2020). Conditional resampling improves sensitivity and specificity of single cell crispr regulatory screens. *bioRxiv*.
- Lam, C., Q. Yao, and N. Bathia (2011). Estimation of latent factors for high-dimensional time series. *Biometrika* 98(4), 901–918.
- Li, G., H. Shen, and J. Z. Huang (2016). Supervised sparse and functional principal component analysis. *Journal of Computational and Graphical Statistics* 25(3), 859–878.
- Lock, E. F. and G. Li (2018). Supervised multiway factorization. *Electronic journal of statistics* 12(1), 1150.
- Lucas, C., P. Wong, J. Klein, T. B. Castro, J. Silva, M. Sundaram, M. K. Ellingson, T. Mao, J. E. Oh, B. Israelow, et al. (2020). Longitudinal analyses reveal immunological misfiring in severe covid-19. *Nature* 584(7821), 463–469.
- Mnih, A. and R. R. Salakhutdinov (2007). Probabilistic matrix factorization. *Advances in neural information processing systems* 20, 1257–1264.
- Phan, A.-H., P. Tichavský, and A. Cichocki (2013). Candecomp/parafac decomposition of high-order tensors through tensor reshaping. *IEEE transactions on signal processing* 61(19), 4847–4860.
- Rendeiro, A. F., J. Casano, C. K. Vorkas, H. Singh, A. Morales, R. A. DeSimone, G. B. Ellsworth, R. Soave, S. N. Kapadia, K. Saito, et al. (2020). Longitudinal immune profiling of mild and severe covid-19 reveals innate and adaptive immune dysfunction and provides an early prediction tool for clinical progression. *medRxiv*.

- Sidiropoulos, N. D., L. De Lathauwer, X. Fu, K. Huang, E. E. Papalexakis, and C. Faloutsos (2017). Tensor decomposition for signal processing and machine learning. *IEEE Transactions on Signal Processing* 65(13), 3551–3582.
- Sorkine, O., D. Cohen-Or, Y. Lipman, M. Alexa, C. Rössl, and H.-P. Seidel (2004). Laplacian surface editing. In *Proceedings of the 2004 Eurographics/ACM SIGGRAPH symposium on Geometry processing*, pp. 175–184.
- Tibshirani, R. (2011). Regression shrinkage and selection via the lasso: a retrospective. *Journal of the Royal Statistical Society: Series B (Statistical Methodology)* 73(3), 273–282.
- Tipping, M. E. and C. M. Bishop (1999). Probabilistic principal component analysis. *Journal of the Royal Statistical Society: Series B (Statistical Methodology)* 61(3), 611–622.
- Wang, D., X. Liu, and R. Chen (2019). Factor models for matrix-valued high-dimensional time series. *Journal of econometrics* 208(1), 231–248.
- Wang, D., Y. Zheng, H. Lian, and G. Li (2021). High-dimensional vector autoregressive time series modeling via tensor decomposition. *Journal of the American Statistical Association*, 1–19.
- Yao, F., H.-G. Müller, and J.-L. Wang (2005). Functional data analysis for sparse longitudinal data. *Journal of the American statistical association* 100(470), 577–590.
- Yokota, T., Q. Zhao, and A. Cichocki (2016). Smooth parafac decomposition for tensor completion. *IEEE Transactions on Signal Processing* 64(20), 5423–5436.